

# Bispectrum from open inflation

Kazuyuki Sugimura,<sup>a</sup> Eiichiro Komatsu<sup>b,c,d</sup>

<sup>a</sup>Yukawa Institute for Theoretical Physics, Kyoto University, Kyoto, Japan

<sup>b</sup>Max-Planck-Institut für Astrophysik, Karl-Schwarzschild Str. 1, 85741 Garching, Germany

<sup>c</sup>Kavli Institute for the Physics and Mathematics of the Universe, Todai Institutes for Advanced Study, the University of Tokyo, Kashiwa, Japan 277-8583 (Kavli IPMU, WPI)

<sup>d</sup>Texas Cosmology Center and the Department of Astronomy, The University of Texas at Austin, 1 University Station, C1400, Austin, TX 78712, USA

E-mail: [sugimura@yukawa.kyoto-u.ac.jp](mailto:sugimura@yukawa.kyoto-u.ac.jp), [komatsu@mpa-garching.mpg.de](mailto:komatsu@mpa-garching.mpg.de)

**Abstract.** We calculate the bispectrum of primordial curvature perturbations,  $\zeta$ , generated during “open inflation.” Inflation occurs inside a bubble nucleated via quantum tunneling from the background false vacuum state. Our universe lives inside the bubble, which can be described as a Friedman-Lemaître-Robertson-Walker (FLRW) universe with negative spatial curvature, undergoing slow-roll inflation. We pay special attention to the issue of an initial state for quantum fluctuations. A “vacuum state” defined by a positive-frequency mode in de Sitter space charted by open coordinates is different from the Euclidean vacuum (which is equivalent to the so-called “Bunch-Davies vacuum” defined by a positive-frequency mode in de Sitter space charted by flat coordinates). Quantum tunneling (bubble nucleation) then modifies the initial state away from the original Euclidean vacuum. While most of the previous study on modifications of the initial quantum state introduces, by hand, an initial time at which the quantum state is modified as well as the form of the modification, an effective initial time naturally emerges and the form is fixed by quantum tunneling in open inflation models. Therefore, open inflation enables a self-consistent computation of the effect of a modified initial state on the bispectrum. We find a term which goes as  $\langle \zeta_{\mathbf{k}_1} \zeta_{\mathbf{k}_2} \zeta_{\mathbf{k}_3} \rangle \propto 1/k_1^2 k_3^4$  in the so-called squeezed configurations,  $k_3 \ll k_1 \approx k_2$ , in agreement with the previous study on modifications of the initial state. The bispectrum in the exact folded limit, e.g.,  $k_1 = k_2 + k_3$ , is also enhanced and remains finite. However, these terms are exponentially suppressed when the wavelength of  $\zeta$  is smaller than the curvature radius of the universe. The leading-order bispectrum is equal to the usual one from single-field slow-roll inflation; the terms specific for open inflation arise only in the sub-leading order when the wavelength of  $\zeta$  is smaller than the curvature radius.

---

## Contents

<b>1</b>	<b>Introduction</b>	<b>1</b>
<b>2</b>	<b>Open inflation</b>	<b>3</b>
<b>3</b>	<b>Quantum field theory for a free scalar field in open inflation</b>	<b>7</b>
<b>4</b>	<b>In-in formalism on a CDL instanton background</b>	<b>11</b>
<b>5</b>	<b>Bispectrum from open inflation</b>	<b>12</b>
5.1	Cubic action in the flat gauge	12
5.2	An example calculation	14
5.3	Bispectrum in the sub-curvature approximation	15
5.3.1	Bispectrum of $\varphi$	15
5.3.2	Bispectrum of $\zeta$	18
<b>6</b>	<b>Conclusion</b>	<b>19</b>
<b>A</b>	<b>Expansion of action in a FLRW universe with negative spatial curvature</b>	<b>20</b>
A.1	Second-order action	21
A.2	Third-order action	21
<b>B</b>	<b>Analytical structure of the universe in open inflation</b>	<b>23</b>
B.1	Coordinate systems and Wightman functions	23
B.2	Deformation of integration path using analyticity	25
<b>C</b>	<b>Order-of-magnitude estimate for sub-leading contributions</b>	<b>27</b>
C.1	Contributions from outside the $R$ -region	27
C.2	Contributions from the sub-leading terms in Lagrangian	28
<b>D</b>	<b>Open harmonics in the sub-curvature approximation</b>	<b>29</b>
D.1	Correspondence with flat harmonics	29
D.2	Correspondence with Fourier modes in flat space	32
D.3	Power spectrum and bispectrum	32

---

## 1 Introduction

“Open inflation” models [1, 2] offer an attractive framework for understanding the origin of our universe. According to this framework, our universe is contained within a single bubble, which was nucleated from a surrounding false vacuum state. This is attractive because there is no physical singularity at the beginning of *our* universe, which is the moment of the bubble nucleation in the de Sitter background. In the simplest scenario worked out by Coleman and De Luccia [3], the metric inside the bubble is a homogeneous and isotropic Friedman-Lemaître-Robertson-Walker (FLRW) metric with negative spatial curvature. Therefore, the

homogeneity and isotropy problems do not exist in this scenario.<sup>1</sup> We still need inflation [4–8] to make geometry of the observable universe sufficiently flat, at the level compatible with observations [9–12]; hence the term, “open inflation.”

How can we test open inflation models? While this is an attractive framework, is it testable/falsifiable? An obvious observable is the spatial curvature of the observable universe. Detection of negative curvature would greatly strengthen the case for open inflation models, while detection of positive curvature would rule them out [13]. In any case, in order for us to have any access to distinct signatures of open inflation, the total number of  $e$ -folds of inflationary expansion must be close to the minimum that is required to make geometry of the observable universe sufficiently flat. If so, we may find signatures of open inflation in scalar [14] and tensor perturbations [15, 16] in temperature anisotropy of the cosmic microwave background (CMB) [17–22].<sup>2</sup> Another possible observable is a signature of other bubbles colliding with ours [28–30].

In this paper, we shall present the first computation of the bispectrum from single-field open inflation.<sup>3</sup> Our model is based on ref. [32], and the potential for the scalar (inflaton) field is shown in figure 1. In these models, a single scalar field is responsible for both quantum tunneling and slow-roll inflation inside the bubble. For simplicity, we shall ignore multi-field effects or the possibility of a rapid-roll era soon after quantum tunneling, although these effects are potentially significant [33, 34]. The bispectrum is the three-point function in Fourier space, and we define it as  $\langle \zeta_{\mathbf{k}_1} \zeta_{\mathbf{k}_2} \zeta_{\mathbf{k}_3} \rangle = (2\pi)^3 \delta_D(\sum_{i=1}^3 \mathbf{k}_i) B(k_1, k_2, k_3)$ , where  $\zeta_{\mathbf{k}}$  is the Fourier transform of a curvature perturbation computed on the uniform density hypersurface.

Our work is motivated in part by recent work on the effects of a modified initial state (non-Bunch-Davies initial state<sup>4</sup>) on the bispectrum [35–43]. In particular, it has been shown that a modified initial state yields an enhanced bispectrum in the so-called squeezed limit, in which one of the wavenumbers is much less than the other two, i.e.,  $k_3 \ll k_1 \approx k_2$ . Specifically,  $B(k, k, k_3) \propto k_3^{-4} k^{-2}$  in the squeezed limit [38–40] instead of the usual  $B(k, k, k_3) \propto k_3^{-3} k^{-3}$  for single-field inflation models with a Bunch-Davies initial state [44]. Such a distinct dependence on  $k_3$  has important implications for observations [45, 46]. However, most of the previous work on a modified initial state puts an initial state at some arbitrary initial time by hand, without specifying its physical origin. The only self-consistent computations that we are aware of use periodic features in the scalar-field potential or kinetic term [47, 48].

In open inflation models, such a modified initial state naturally emerges as a result of the evolution from the Euclidean vacuum (which is equivalent to the Bunch-Davies vacuum in de Sitter space charted by flat coordinates) via quantum tunneling [18, 49, 50]. Therefore, open inflation enables a self-consistent computation of the effect of a modified initial state on the bispectrum.

This paper is organized as follows. In section 2, we review open inflation and our coordinate system. In section 3, we review quantum field theory for a free scalar field in open inflation. In section 4, we outline the in-in formalism on a Coleman-De Luccia instanton background, with which we calculate the bispectrum in section 5. Finally, we conclude in

<sup>1</sup>However, one may argue that this is merely a consequence of the assumptions made in the analysis of Coleman and De Luccia, who studied a bubble nucleation in a homogeneous and isotropic background.

<sup>2</sup>See refs. [23–27] for earlier calculations based upon a conformal vacuum state (rather than the Euclidean vacuum state we shall work with in this paper).

<sup>3</sup>See ref. [31] for related work on the bispectrum from inflation with positive spatial curvature.

<sup>4</sup>We shall define what we mean by the “Bunch-Davies initial state” in section 3.

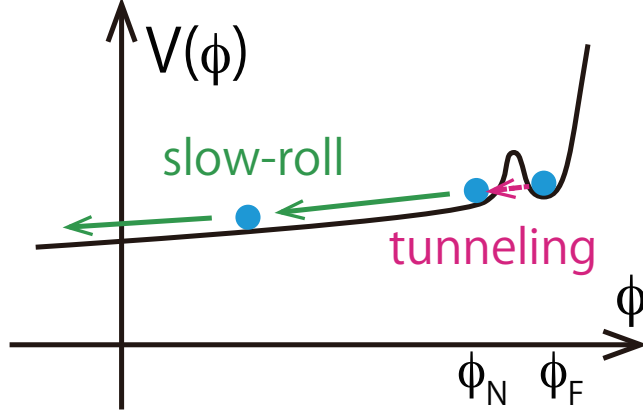


**Figure 1.** Potential for single-field open inflation. Slow-roll inflation begins after a scalar field tunneling from the false vacuum state,  $\phi_F$ , to the nucleation point,  $\phi_N$ . The essential features of this potential are: the potential heights before and after tunneling are approximately the same,  $V(\phi_F) \approx V(\phi_N)$ ; the barrier height is small compared to  $V(\phi_F)$ ; and the barrier is narrow,  $V \ll |d^2V/d\phi^2|$  at the barrier.

section 6. In appendix A, we derive the second- and third-order actions for scalar perturbations. In appendix B, we show how we choose the paths of integration when computing the correlation function. In appendix C, we show that all but one term in the third-order action after field redefinition is important in the sub-curvature approximation. In appendix D, we show the correspondence between the open harmonics and the Fourier modes in flat space in the sub-curvature approximation.

We adopt the units  $c = \hbar = 8\pi G = 1$ .

## 2 Open inflation

We describe quantum tunneling using a Coleman-De Luccia (CDL) instanton,  $\bar{\phi}(x)$  and  $\bar{g}_{\mu\nu}(x)$  [3]. A CDL instanton, which is an Euclidean  $O(4)$ -symmetric solution, can be written as a function of only one variable,  $\bar{\phi}(\tau)$  and  $\bar{a}(\tau)$ , where  $\tau$  is the imaginary (Euclidean) time. We study quantum tunneling using the Euclidean metric given by

$$ds^2 = d\tau^2 + \bar{a}^2(\tau)(d\chi^2 + \sin^2\chi d\Omega^2), \quad (2.1)$$

with  $d\Omega^2$  being the metric of a 2-sphere ( $S_2$ ). We then analytically continue the solution beyond tunneling (i.e., bubble nucleation) in order to describe the post-tunneling world.

The equations of motion (EOMs) for the instanton are given by

$$\frac{d^2\bar{\phi}(\tau)}{d\tau^2} + 3\frac{d\ln\bar{a}(\tau)}{d\tau}\frac{d\bar{\phi}(\tau)}{d\tau} - \frac{dV[\bar{\phi}(\tau)]}{d\bar{\phi}} = 0, \quad (2.2)$$

$$\left[\frac{d\ln\bar{a}(\tau)}{d\tau}\right]^2 = -\frac{V[\bar{\phi}(\tau)]}{3} + \frac{1}{\bar{a}^2(\tau)}, \quad (2.3)$$

where the potential,  $V(\phi)$ , has a false vacuum at  $\phi_F$ . We have a slow-roll inflation phase following the quantum tunneling to a nucleation point,  $\phi_N$  (see figure 1).

For simplicity, we shall assume that the potential barrier is small compared with the vacuum energy of the false vacuum, and the potential heights before and after tunneling as well as during the subsequent slow-roll phase are approximately equal, i.e.,  $V(\phi_F) \approx V(\phi_N) \approx V(\phi_I) \equiv V_I$ , where  $\phi_I$  denotes the scalar field values during slow-roll inflation. Then, we can approximate  $V(\phi)$  as  $V(\phi) \approx V_I$  in eq. (2.3), and  $\bar{a}$  is approximately given by the scale factor of Euclidean de Sitter spacetime,

$$\bar{a}(\tau) = \frac{1}{H_I} \sin(H_I \tau), \quad (2.4)$$

with  $H_I^2 = V_I/3$ . With this choice of coordinates  $\tau$ , the two ends of the Euclidean 4-sphere in  $\tau$  correspond to  $H_I \tau = \pm\pi/2$ . The boundary conditions for the instanton are  $d\bar{\phi}(\tau)/d\tau = 0$  at  $\tau = \pm\pi/(2H_I)$ . We shall also assume that the potential barrier is narrow,  $H_I^2 \ll |d^2V/d\phi^2|$ .

With these assumptions,  $\bar{\phi}$  is approximately given by a thin-wall instanton solution:

$$\bar{\phi}(\tau) \approx \begin{cases} \phi_F & \left(-\frac{\pi}{2H_I} \leq \tau < \frac{\pi}{2H_I} - R_W\right) \\ \phi_N & \left(\frac{\pi}{2H_I} - R_W < \tau \leq \frac{\pi}{2H_I}\right) \end{cases}, \quad (2.5)$$

where  $R_W$  is the radius of the bubble wall.

The world after bubble nucleation can be described by analytical continuation of a CDL instanton to Lorentzian regions. For the Euclidean de Sitter spacetime defined by eq. (2.4), analytical continuation is made with the following coordinate system [51],

$$E_1\text{- and } E_2\text{-regions: } \begin{cases} \tau & (-\pi/(2H_I) \leq \tau \leq \pi/(2H_I)), \\ \chi & (0 \leq \chi \leq \pi), \end{cases} \quad (2.6)$$

$$R\text{-region: } \begin{cases} t_R = i(\tau - \pi/(2H_I)) & (0 \leq t_R < \infty), \\ r_R = i\chi & (0 \leq r_R < \infty), \end{cases} \quad (2.7)$$

$$L\text{-region: } \begin{cases} t_L = i(-\tau - \pi/(2H_I)) & (0 \leq t_L < \infty), \\ r_L = i\chi & (0 \leq r_L < \infty), \end{cases} \quad (2.8)$$

$$C\text{-region: } \begin{cases} t_C = \tau & (-\pi/(2H_I) \leq t_C \leq \pi/(2H_I)), \\ r_C = i(\chi - \frac{\pi}{2}) & (0 \leq r_C < \infty). \end{cases} \quad (2.9)$$

The  $E_1$ - and  $E_2$ -regions are the original Euclidean regions we have used to describe quantum tunneling, which consist of two 4-hemispheres  $E_1$  and  $E_2$  defined by  $0 \leq \chi < \pi/2$  (“north”) and  $\pi/2 < \chi \leq \pi$  (“south”), respectively. The others are the Lorentzian regions, which describe the world after quantum tunneling. Each region and its physical meaning are illustrated in figure 2. The coordinates of a 2-sphere,  $\Omega^i$ , are commonly used for all regions. The boundaries between the  $C$ - and  $R$ -regions and the  $C$ - and  $L$ -regions are coordinate singularities.

With the coordinate system given in eq. (2.6) to (2.9), the metrics in the  $E$ -,  $R$ -,  $L$ -, and  $C$ -regions are given, respectively, by

$$\begin{aligned} ds^2 &= d\tau^2 + H_I^{-2} \cos^2 H_I \tau (d\chi^2 + \sin^2 \chi d\Omega^2) \\ &= -dt_R^2 + H_I^{-2} \sinh^2 H_I t_R (dr_R^2 + \sinh^2 r_R d\Omega^2) \\ &= -dt_L^2 + H_I^{-2} \sinh^2 H_I t_L (dr_L^2 + \sinh^2 r_L d\Omega^2) \\ &= dt_C^2 + H_I^{-2} \cos^2 H_I t_C (-dr_C^2 + \cosh^2 r_C d\Omega^2), \end{aligned} \quad (2.10)$$

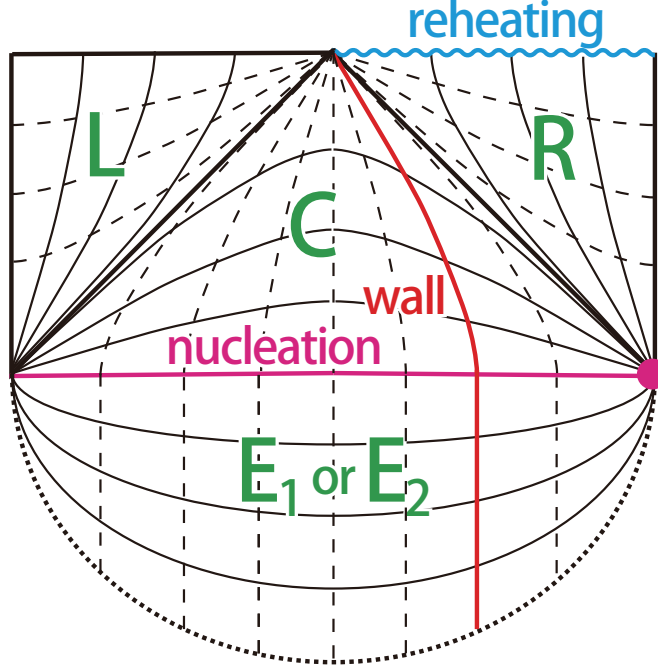


**Figure 2.** Penrose-like diagram of open inflation. The top half (above the line labeled “nucleation”) corresponds to the world after bubble nucleation, and the time is real. The bottom half corresponds to either one of the two hemispheres of the Euclidean 4-sphere,  $E_1$  (“north”) or  $E_2$  (“south”), and the time is imaginary. (Also see figure 3.) The solid and dashed lines show  $r = \text{constant}$  and  $t = \text{constant}$  lines, respectively, in the  $R$ -,  $L$ -, and  $C$ -regions, while they show  $\chi = \text{constant}$  and  $\tau = \text{constant}$ , respectively, in the  $E_1$ - and  $E_2$ -regions. The  $R$ -region describes the interior of the bubble, i.e., our universe. The  $C$ -region contains a worldline of the bubble wall, which separates the interior (located to the right of the line labeled “wall”) and exterior of the bubble. The exterior of the bubble is in the false vacuum state with  $\bar{\phi} = \phi_F$ . The big filled circle at the right edge of the line labeled “nucleation” shows the location of the bubble center at the time of nucleation. Note that the bubble has a finite size upon nucleation. The  $L$ -region is in the false vacuum state with  $\bar{\phi} = \phi_F$ . The coordinate values are chosen such that the right vertical edge of the  $R$ -region has  $r_R = 0$ , and the thick solid line between the  $R$ - and  $C$ -regions have  $t_R = 0$  and  $r_R = \infty$  as well as  $t_C = \pi/(2H_I)$  and  $r_C = \infty$ . The line labeled “nucleation” has  $r_C = 0$  as well as  $\chi = \pi/2$ . The left vertical edge of the  $L$ -region has  $r_L = 0$ , and the thick solid line between the  $L$ - and  $C$ -regions have  $t_L = 0$  and  $r_L = \infty$  as well as  $t_C = -\pi/(2H_I)$  and  $r_C = \infty$ . Finally, while the top edge of the  $L$ -region has  $t_L = \infty$ , that of the  $R$ -region is somewhat fuzzy because slow-roll inflation in the  $R$ -region must end in a finite time and our universe must enter a radiation-dominated era after reheating (which is not shown in this diagram). While  $t$  and  $r$  in the  $R$ - and  $L$ -regions coincide with the familiar time and radial coordinates in a FLRW universe, those in the  $C$ -region do not. For example, a  $t_C = \text{constant}$  line gives a worldline of a body with constant acceleration (which is analogous to the Rindler coordinates). Therefore, the bubble wall in the  $C$ -region is accelerated and its worldline approaches a null line as  $r_C \rightarrow \infty$ . In this paper, the wall worldline is along  $t_C = R_W$  where  $R_W$  is the radius of the bubble, and  $\phi(t_C) = \phi_F$  and  $\phi_N$  for  $-\pi/(2H_I) \leq t_C < \pi/(2H_I) - R_W$  (exterior of the bubble) and  $\pi/(2H_I) - R_W < t_C \leq \pi/(2H_I)$  (interior), respectively (eq. (2.5)).

and  $\phi$ 's in the corresponding regions are given, respectively, by

$$\phi(\tau) = \bar{\phi}(\tau), \quad (2.11)$$

$$\phi(t_R) = \bar{\phi}[-it_R + \pi/(2H_I)], \quad (2.12)$$

$$\phi(t_L) = \bar{\phi}[it_L - \pi/(2H_I)], \quad (2.13)$$

$$\phi(t_C) = \bar{\phi}(t_C), \quad (2.14)$$

where  $\bar{\phi}(\tau)$  is a solution to eqs. (2.2) and (2.3).

We live in the future of the  $R$ -region, in which slow-roll inflation occurs after quantum tunneling, and reheating follows after inflation (see figure 2). In the  $R$ -region, a  $t_R = \text{const}$  surface is both a 3-hyperboloid and a  $\phi = \text{const}$  surface; thus, we observe the  $R$ -region as a FLRW universe with negative spatial curvature.

If we could solve eqs. (2.2) and (2.3) exactly for a given potential written by an analytical function, analytical continuation given by eq. (2.7) to (2.9) would give a complete description of the world after quantum tunneling. However, since the solutions given in eqs. (2.4) and (2.5) are approximation, we need to re-solve the EOM for  $\phi$  and the Friedmann equation in a FLRW universe with negative spatial curvature, in order to describe the evolution of the universe in the region where the solutions given in eqs. (2.4) and (2.5) are not valid. We shall therefore use eqs. (2.4) and (2.5) as the initial conditions for the subsequent evolution of  $\phi(t)$  and  $a(t)$ .

For brevity, in the following we omit the subscript  $R$  from  $t_R$  and  $r_R$  unless otherwise stated. The metric in the  $R$ -region is given by

$$ds^2 = -dt^2 + a^2(t)\gamma_{ij}dx^i dx^j, \quad (2.15)$$

where  $\gamma_{ij}$  is the metric for the unit 3-hyperboloid given by

$$\gamma_{ij}dx^i dx^j \equiv dr^2 + \sinh^2 r d\Omega^2, \quad (2.16)$$

and  $a(t)$  is the FLRW scale factor. The EOM for  $\phi$  and the Friedmann equation are given, respectively, by

$$\ddot{\phi}(t) + 3H(t)\dot{\phi}(t) + \frac{dV[\phi(t)]}{d\phi} = 0, \quad (2.17)$$

$$H^2(t) = \frac{V[\phi(t)]}{3} + \frac{1}{a^2(t)}, \quad (2.18)$$

where the over-dots denote derivatives with respect to  $t$  and  $H(t) \equiv \dot{a}(t)/a(t)$  is in general different from  $H_I$ . The initial conditions are given by  $a(0) = 0$ ,  $\dot{a}(0) = 1$ ,  $\phi(0) = \phi_N$ , and  $\dot{\phi}(0) = 0$ , according to the CDL instanton solution.

At the onset of slow-roll inflation in the  $R$ -region, the universe is still in a curvature-dominated era, i.e., the spatial curvature term is still dominant in the Friedmann equation. However, spatial curvature decays away as the universe expands, and an inflationary era begins when the potential of  $\phi$  becomes dominant in the Friedmann equation. After reaching the inflationary era, the universe evolves in the same way as the usual slow-roll inflation scenario. We thus impose slow-roll conditions:

$$\epsilon \equiv \frac{(dV/d\phi)^2}{2V^2} \ll 1, \quad \epsilon_\eta \equiv \frac{(d^2V/d^2\phi)}{V} \ll 1. \quad (2.19)$$



Although the slow-roll conditions may be broken during the curvature-dominated era, we shall assume that the slow-roll conditions are satisfied in the whole  $R$ -region.

Let us define the conformal time,  $\eta \equiv \int_{\infty}^t dt'/a(t')$ . To the leading order of the slow-roll parameters, we have  $\eta \approx -(1/2) \log((\cosh H_I t + 1)/(\cosh H_I t - 1))$ . The curvature-dominated era and the inflationary era correspond approximately to  $-\infty < \eta \lesssim -1$  and  $-1 \lesssim \eta < 0$ , respectively. The scale factor and the Hubble parameter are approximately given by

$$a(\eta) \approx \begin{cases} \frac{e^\eta}{2H_I} & (-\infty < \eta \lesssim -1) \\ -\frac{1}{H_I \eta} & (-1 \lesssim \eta < 0) \end{cases}, \quad H(\eta) \approx \begin{cases} -H_I \eta & (-\infty < \eta \lesssim -1) \\ H_I & (-1 \lesssim \eta < 0) \end{cases}. \quad (2.20)$$

The first and second derivatives of the scalar field with respect to time are approximately given by

$$\dot{\phi}(\eta) \approx \begin{cases} -\frac{3\sqrt{2}\epsilon}{2} H_I e^\eta & (-\infty < \eta \lesssim -1) \\ -\sqrt{2}\epsilon H_I & (-1 \lesssim \eta < 0) \end{cases}, \quad \ddot{\phi}(\eta) \approx \begin{cases} -\frac{3\sqrt{2}\epsilon}{4} H_I^2 & (-\infty < \eta \lesssim -1) \\ \sqrt{2}\epsilon(\epsilon + \epsilon_\eta) H_I^2 & (-1 \lesssim \eta < 0) \end{cases}. \quad (2.21)$$

We assume that the potential is a monotonically increasing function of  $\phi$  (except for the barrier), and thus  $\dot{\phi}$  and  $\ddot{\phi}$  have definite signs.

### 3 Quantum field theory for a free scalar field in open inflation

In this section, we review quantum field theory (QFT) for a free scalar field in open inflation [18, 49, 50]. Hereafter, we shall consider only scalar-type perturbations. We write the perturbed scalar field around the uniform background,  $\phi(t)$ , as

$$\phi(t, \mathbf{x}) = \phi(t) + \varphi(t, \mathbf{x}), \quad (3.1)$$

where  $\varphi$  is the scalar field perturbation. We write the spatial coordinates as  $\mathbf{x} \equiv (r, \Omega)$  for brevity. From now on, we shall use  $\phi$  to denote the background scalar field,  $\phi(t)$ , unless otherwise stated.

The perturbed metric in the  $R$ -region around the metric given by eq. (2.15) is written in the Arnowitt-Deser-Misner (ADM) form as [52]

$$ds^2 = -N^2 dt^2 + h_{ij} (dx^i + N^i dt) (dx^j + N^j dt), \quad (3.2)$$

where  $h_{ij} = a^2(t) e^{2\zeta} \gamma_{ij}$  is the spatial metric with the curvature perturbation  $\zeta$ ,  $N$  the lapse function, and  $N_i$  the shift vector. We fix the gauge degrees of freedom by taking the uniform curvature (flat) gauge,  $\zeta \equiv 0$ , and obtain the quadratic action for scalar perturbations by substituting the constraint equations into the original action. As we show in appendix A.1, the quadratic action for scalar perturbations up to the leading order in the slow-roll parameters is given by

$$S_2 \left( \equiv \int d^4 x \mathcal{L}_0 \right) = \int dt d^3 \mathbf{x} a^3 \sqrt{\gamma} \left[ \frac{1}{2} \dot{\varphi}^2 - \frac{1}{2a^2} \partial_i \varphi \partial^i \varphi \right], \quad (3.3)$$



where  $\mathcal{L}_0$  is the Lagrangian density for free theory,  $\partial_i$  denotes 3-dimensional covariant derivatives with respect to  $\gamma_{ij}$ , and  $\partial^i$  is defined by  $\partial^i \equiv \gamma^{ij} \partial_j$ . eq. (3.3), derived in the  $R$ -region, can also be used outside the  $R$ -region by analytical continuation, except near the bubble wall, for which a non-zero mass term should be inserted into the action.

Next, we obtain the 2-point function of  $\varphi$ . We promote  $\varphi$  to an operator,  $\hat{\varphi}$ , and write

$$\hat{\varphi}(x) = \sum_{\mathbf{k}} \left[ u_{\mathbf{k}}(x) \hat{a}_{\mathbf{k}} + v_{\mathbf{k}}(x) \hat{a}_{\mathbf{k}}^\dagger \right], \quad (3.4)$$

where  $\hat{a}_{\mathbf{k}}$  and  $\hat{a}_{\mathbf{k}}^\dagger$  are the annihilation and creation operators, respectively, that satisfy the commutation relation,  $[\hat{a}_{\mathbf{k}}, \hat{a}_{\mathbf{k}'}^\dagger] = \delta_{\mathbf{k}\mathbf{k}'}$ ; and  $u_{\mathbf{k}}(x)$  and  $v_{\mathbf{k}}(x)$  are mode functions, which form a complete set. The mode functions are solutions of the linearized EOMs. Whilst  $v_{\mathbf{k}}(x) = u_{\mathbf{k}}^*(x)$  in the Lorentzian region, the same relation does not necessarily hold in the Euclidean region, as the argument  $x$  may contain an imaginary part.

The choice of  $u_{\mathbf{k}}$  selects a “vacuum state,”  $|0\rangle$ , which is annihilated by the annihilation operator in eq. (3.4),  $\hat{a}_{\mathbf{k}}|0\rangle = 0$ . The most natural choice of a vacuum state in de Sitter space is the Euclidean vacuum,  $|0_E\rangle$ . The Euclidean vacuum is defined by a purely positive-frequency function which is analytical in  $E_2$ . The two-point function (Wightman function) computed with respect to this vacuum state,  $\langle 0_E | \varphi(x) \varphi(x') | 0_E \rangle$ , is invariant under de Sitter group  $\text{SO}(4,1)$  (see section 5.4 of ref. [53]).<sup>5</sup>

However, a positive-frequency function of de Sitter space charted by open coordinates does not give a purely positive-frequency function of the Euclidean vacuum state. This is not a surprise: a positive-frequency function defined in a given coordination is typically a mixture of positive- and negative-frequency functions defined in another coordination, and the relation between them is given by the Bogoliubov transformation. For example, a positive-frequency function of Minkowski space charted by Rindler coordinates is a mixture of positive- and negative-frequency functions of Minkowski space charted by  $ds^2 = -dt^2 + d\mathbf{x}^2$  (whose positive-frequency function defines the Minkowski vacuum), and thus a comoving Rindler observer (who experiences a constant acceleration in Minkowski space) detects particles (see section 4.5 of ref. [53]).

Sasaki, Tanaka, and Yamamoto derive an appropriate mixture of positive- and negative-frequency functions of de Sitter space charted by open coordinates, whose annihilation operator annihilates the Euclidean vacuum [51]. They expand  $\hat{\varphi}$  as

$$\hat{\varphi}(x) = \sum_{plm} \sum_{\sigma=\pm} \left[ u_{plm}^{(\sigma)}(x) \hat{a}_{plm}^{(\sigma)} + v_{plm}^{(\sigma)}(x) \hat{a}_{plm}^{(\sigma)\dagger} \right], \quad (3.5)$$

with  $\hat{a}_{plm}^{(\sigma)}|0_E\rangle = 0$  for  $\sigma = \pm$ . The mode functions,  $u_{plm}^{(\sigma)}$  ( $v_{plm}^{(\sigma)}$ ), are chosen to be analytical in  $E_2$  ( $E_1$ ); hence the Euclidean vacuum. They are linear combinations of positive- and negative-frequency functions defined in the  $R$  and  $L$  regions.

---

<sup>5</sup>The Euclidean vacuum state is equivalent to the Bunch-Davies vacuum state [54], which is perhaps more familiar to cosmologists. The Bunch-Davies state is defined by a positive-frequency function of de Sitter space charted by flat coordinates. Specifically, for flat coordinates of  $ds^2 = a^2(\eta)(-d\eta^2 + d\mathbf{x}^2)$  with  $a(\eta) = -1/(H\eta)$ , a positive-frequency function for a minimally-coupled scalar field with mass  $m$  is given by the Hankel function of the first kind as  $u_{\mathbf{k}} = \frac{\sqrt{-\pi\eta}}{2(2\pi)^{3/2}a} H_{\nu}^{(1)}(-k\eta) e^{i\mathbf{k}\cdot\mathbf{x}}$  with  $\nu^2 = \frac{9}{4} - \frac{m^2}{H^2}$  for  $\eta < 0$ . This function is analytical in the entire lower half complex  $\eta$  plane [ $\text{Im}(\eta) < 0$ ], and  $u_{\mathbf{k}}$  is finite in the limit of  $\eta \rightarrow -(1+i\epsilon)\infty$ . This procedure yields a purely positive-frequency function of the Euclidean vacuum state. The annihilation operator defined with respect to this  $u_{\mathbf{k}}$  annihilates the Euclidean vacuum,  $\hat{a}_{\mathbf{k}}|0_E\rangle = 0$ , and a comoving observer in de Sitter space charted by flat coordinates does not detect particles (see section 5.4 of ref. [53]; also see ref. [55]).

They then write the mode functions as  $u_{plm}^{(\sigma)}(x) = u_p^{(\sigma)}(\eta)Y_{plm}(\mathbf{x})$ , where  $Y_{plm}(\mathbf{x})$  are harmonics on a 3-hyperboloid, and the indices  $p, l$ , and  $m$  take on  $0 < p < \infty, l = 0, 1, 2 \dots$ , and  $m = -l, -l + 1, \dots, l - 1, l$ , respectively. The explicit form is given by  $Y_{plm}(\mathbf{x}) = f_{pl}(r)Y_{lm}(\Omega)$ , where  $Y_{lm}(\Omega)$  is the spherical harmonics on a 2-sphere, and [51]

$$f_{pl}(r) = \left| \frac{\Gamma(ip + l + 1)}{\Gamma(ip + 1)} \right| \frac{p}{\sqrt{\sinh r}} P_{ip-1/2}^{-l-1/2}(\cosh r), \quad (3.6)$$

with  $P_\mu^\nu(z)$  being the associated Legendre functions. This function goes as  $f_{pl}(r) \propto e^{-r}$  for  $p^2 > 0$ , and  $r = 1$  corresponds to the curvature radius of a 3-hyperboloid. Therefore, the modes with  $p^2 > 0$  decay exponentially on scales larger than the curvature radius, and represent “sub-curvature modes.” In this paper, we shall consider the modes with  $p^2 > 0$  only, and ignore “super-curvature modes” [56, 57], which are described by the modes with  $p^2 < 0$ . This is justified at the tree level: current observations suggest that the curvature radius is greater than our current horizon size, and the modes within our horizon are not affected by super-horizon modes at the tree level. The harmonics satisfy the following relations:

$$\begin{aligned} \partial^2 Y_{plm}(\mathbf{x}) &= -(p^2 + 1)Y_{plm}(\mathbf{x}), \\ Y_{plm}^*(\mathbf{x}) &= (-1)^m Y_{pl-m}(\mathbf{x}), \\ \int d^3\mathbf{x} \sqrt{\gamma} Y_{p_1 l_1 m_1}^*(\mathbf{x}) Y_{p_2 l_2 m_2}(\mathbf{x}) &= \delta(p_1 - p_2) \delta_{l_1 l_2} \delta_{m_1 m_2}, \\ \int_0^\infty dp \sum_{lm} Y_{plm}^*(\mathbf{x}) Y_{plm}(\mathbf{x}') &= \delta^{(3)}(\mathbf{x} - \mathbf{x}'). \end{aligned} \quad (3.7)$$

The conformal-time dependence of the mode function for a massless minimally-coupled scalar field,  $u_p^{(\sigma)}(\eta)$ , is given by [51]

$$u_p^{(\sigma)}(\eta) = \frac{1}{\sqrt{2(1 - e^{-2\pi p})}} \tilde{u}_p(\eta) - \sigma \frac{e^{-\pi p}}{\sqrt{2(1 - e^{-2\pi p})}} \tilde{v}_p(\eta) \quad (3.8)$$

with

$$\tilde{u}_p(\eta) = H_I \frac{\cosh \eta + ip \sinh \eta}{\sqrt{2p(1 + p^2)}} e^{-ip\eta}, \quad \tilde{v}_p(\eta) = H_I \frac{\cosh \eta - ip \sinh \eta}{\sqrt{2p(1 + p^2)}} e^{ip\eta}. \quad (3.9)$$

As  $\tilde{u}_p$  and  $\tilde{v}_p$  are positive- and negative-frequency functions naturally defined in the  $R$ -region (recall that eq. (3.9) is written in coordinates in the  $R$ -region), a comoving observer in the  $R$ -region detects particles with respect to the Euclidean vacuum. To see this, let us expand  $\hat{\varphi}$  in the  $R$ -region as  $\hat{\varphi}(x) = \sum_{plm} [\tilde{u}_p(\eta) Y_{plm}(\mathbf{x}) \tilde{a}_{plm} + \tilde{v}_p(\eta) Y_{plm}^*(\mathbf{x}) \tilde{a}_{plm}^\dagger]$ . Then, the occupation number of particles is given by

$$N_{plm} = \langle 0_E | \tilde{a}_{plm}^\dagger \tilde{a}_{plm} | 0_E \rangle = \frac{1}{e^{2\pi p} - 1}, \quad (3.10)$$

which is a thermal spectrum. The argument and result given here basically parallel those for particle creation in Rindler space, i.e., a comoving observer in Rindler space sees particles with a thermal spectrum (see eq. (4.97) of ref. [53]).

The Euclidean vacuum state given by eq. (3.8) is a natural choice for quantum fluctuations in homogeneous de Sitter space before bubble nucleation. The initial state then

evolves away from the Euclidean vacuum state via bubble nucleation; thus, eq. (3.8) must be modified. In the  $R$ -region, we find  $u_{\mathbf{k}}(x)$  by solving the following linearized EOM,

$$\frac{\delta L}{\delta \varphi} \equiv -\ddot{\varphi}(x) - 3H(t)\dot{\varphi}(x) + \frac{1}{a^2(t)}\partial^2\varphi(x) = 0, \quad (3.11)$$

where  $\partial^2 \equiv \gamma^{ij}\partial_i\partial_j$ , and  $L$  is given by  $S_2 = \int d^4x a^3 \sqrt{\gamma} L$ , and is also related to the Lagrangian density,  $\mathcal{L}$ , by  $\mathcal{L} = a^3 \sqrt{\gamma} L$ . This EOM is obtained by the variation of the second order action given in eq. (3.3). For our model, we can choose the mode functions such that one vanishes in the  $R$ -region and another vanishes in the  $L$ -region [18]. Specifically, we expand  $\hat{\varphi}$  as

$$\hat{\varphi}(x) = \sum_{plm} \left[ u_{plm}^R(x) \hat{a}_{plm}^R + v_{plm}^R(x) \hat{a}_{plm}^{R\dagger} + u_{plm}^L(x) \hat{a}_{plm}^L + v_{plm}^L(x) \hat{a}_{plm}^{L\dagger} \right], \quad (3.12)$$

where  $u_{plm}^R$  and  $u_{plm}^L$  vanish in the  $L$ - and  $R$ -regions, respectively. (Similarly for  $v_{plm}^R$  and  $v_{plm}^L$ .) In this paper, we shall consider  $u_{plm}^R$  (and  $v_{plm}^R$ ) only, as we have no access to the  $L$ -region observationally; henceforth we shall drop the superscript  $R$ , i.e.,  $u_{plm}^R \rightarrow u_{plm}$  and  $v_{plm}^R \rightarrow v_{plm}$ , unless stated otherwise. We then write

$$u_{plm}(x) = u_p(\eta) Y_{plm}(\mathbf{x}). \quad (3.13)$$

Yamamoto, Sasaki, and Tanaka find [18]

$$u_p(\eta) = \frac{1}{\sqrt{1 - e^{-2\pi p}}} \tilde{u}_p(\eta) + \frac{e^{-\pi p - 2i\delta_p}}{\sqrt{1 - e^{-2\pi p}}} \tilde{v}_p(\eta), \quad (3.14)$$

with  $\tilde{u}_p(\eta)$  and  $\tilde{v}_p(\eta)$  given by eq. (3.9).<sup>6</sup> Unlike the previous mode function given in eq. (3.8), the annihilation operator defined with respect to eq. (3.14) does *not* annihilate the Euclidean vacuum. Again,  $\tilde{u}_p$  and  $\tilde{v}_p$  are positive- and negative-frequency functions naturally defined in the  $R$ -region; thus, writing  $\hat{\varphi}(x) = \sum_{plm} [\tilde{u}_p(\eta) Y_{plm}(\mathbf{x}) \tilde{a}_{plm} + \tilde{v}_p(\eta) Y_{plm}^*(\mathbf{x}) \tilde{a}_{plm}^\dagger]$  in the  $R$ -region, we find that the occupation number of particles detected in the  $R$ -region with respect to the new vacuum state,  $|0\rangle$ , is still given by a thermal spectrum,  $N_{plm} = \langle 0 | \tilde{a}_{plm}^\dagger \tilde{a}_{plm} | 0 \rangle = (e^{2\pi p} - 1)^{-1}$ .

As a comoving observer in the  $R$ -region, which is inside the nucleated bubble, detects particles (also see ref. [58] which discusses particle creation due to bubble nucleation in Minkowski space), the state for quantum fluctuations set at the time of bubble nucleation in open inflation is a *non*-Bunch-Davies vacuum state.

With the definition of the field operator given in eq. (3.12), the Wightman functions,  $G^\pm(x, x')$ , are given by

$$\begin{aligned} G^+(x, x') &\equiv \langle 0 | \varphi(x) \varphi(x') | 0 \rangle = \sum_{plm} [u_{plm}^R(x) v_{plm}^R(x') + u_{plm}^L(x) v_{plm}^L(x')] , \\ G^-(x, x') &\equiv \langle 0 | \varphi(x') \varphi(x) | 0 \rangle = \sum_{plm} [u_{plm}^R(x') v_{plm}^R(x) + u_{plm}^L(x') v_{plm}^L(x)] . \end{aligned} \quad (3.15)$$

---

<sup>6</sup>Here, we do not give the explicit expression for the complex phase,  $\delta_p$ , which does not affect the conclusion of this paper (see ref. [18] for the way to obtain  $\delta_p$ ). While eq. (3.14) is written with the coordinates in the  $R$ -region, analytical continuation lets us use it also in parts of the  $C$ - and  $E$ -regions which are inside the bubble.

While  $G^+(x, x') = G^-(x, x') (\equiv G(x, x'))$  for space-like separated  $x$  and  $x'$ ,  $G^+(x, x')$  and  $G^-(x, x')$  are different for time-like separated  $x$  and  $x'$ .

Let us now calculate the power spectrum. The multipole expansion coefficients of  $\varphi$  are defined by

$$\varphi_{plm}(\eta) = \int d^3\mathbf{x} \sqrt{\gamma} Y_{plm}^*(\mathbf{x}) \varphi(\eta, \mathbf{x}) , \quad (3.16)$$

and the power spectrum,  $P(p)$ , is defined by  $\langle \varphi_{plm}^* \varphi_{p'l'm'} \rangle = \delta(p - p') \delta_{ll'} \delta_{mm'} P(p)$ . From eqs. (3.4), (3.7), (3.14), and (3.16),  $P(p)$  at late time (i.e.,  $\eta \approx 0$ ) is given by [18]

$$P(p) = H_I^2 \frac{\cosh \pi p + \cos 2\delta_p}{2p(1 + p^2) \sinh \pi p} . \quad (3.17)$$

We recover a scale-invariant spectrum in the large  $p$  limit,  $P(p) \rightarrow H_I^2/(2p^3)$ . This is an expected result, as large- $p$  modes do not feel curvature of space, and the occupation number of particles falls off exponentially at large  $p$ .

#### 4 In-in formalism on a CDL instanton background

Here, we outline the in-in formalism on a CDL instanton background, which can be used to calculate the bispectrum in open inflation models. The formalism is a natural extension of the in-in formalism in de Sitter space charted by flat coordinates [44] to the case of a universe with quantum tunneling. The free QFT in open inflation, as reviewed in section 3, is based on a WKB analysis of a tunneling wave function without non-linear interaction terms [59–61]. By performing a similar analysis with interaction terms, the in-in formalism can be extended to the case of open inflation [62–64].

The Lagrangian density is given by

$$\mathcal{L}_{full} = \mathcal{L}_0 + \mathcal{L}_{int} , \quad (4.1)$$

where  $\mathcal{L}_0$  and  $\mathcal{L}_{int}$  are the free and interaction parts of the Lagrangian density, respectively. Non-trivial time evolution in  $\mathcal{L}_0$  causes the state to evolve away from the Bunch-Davies vacuum state, and  $\mathcal{L}_{int}$  is a source of non-Gaussianity. The in-in formalism on a CDL instanton background tells us that the  $N$ -point function of  $\varphi$  for  $x_i$ s on a spacial hypersurface  $\Sigma_0$  is given by

$$\langle \varphi(x_1) \varphi(x_2) \cdots \varphi(x_N) \rangle = \frac{\langle 0 | P \varphi(x_1) \varphi(x_2) \cdots \varphi(x_N) e^{i \int_{C \times \Sigma_\lambda} d\lambda d^3\mathbf{x} \mathcal{L}_{int}(x)} | 0 \rangle}{\langle 0 | P e^{i \int_{C \times \Sigma_\lambda} d\lambda d^3\mathbf{x} \mathcal{L}_{int}(x)} | 0 \rangle} , \quad (4.2)$$

where the  $\lambda$  integral is performed along the path  $C = C_1 + C_2$ , and the  $\mathbf{x}$  integral is over the hypersurface  $\Sigma_\lambda$  for a given  $\lambda$  (see figure 3). The path ordering operator,  $P$ , orders operators in the expression according to the order along  $C$ . Covariance of eq. (4.2) guarantees that the  $N$ -point function is not affected by the choice of  $C$  or  $\Sigma_\lambda$ .

The path of integration is shown in figure 3. In the first integration domain,  $V_1 \equiv C_1 \times \Sigma_\lambda$  (the green arrows), the path  $C_1$  starts in  $E_1$  and runs through the nucleation surface  $\Sigma_N$  to  $\Sigma_0$ . In the second domain,  $V_2 \equiv C_2 \times \Sigma_\lambda$  (the red arrows), the path  $C_2$  starts from  $\Sigma_0$  and runs through  $\Sigma_N$  into  $E_2$ . The contributions to the integral from the Euclidean and Lorentzian regions correspond to contributions from during and after bubble nucleation, respectively.

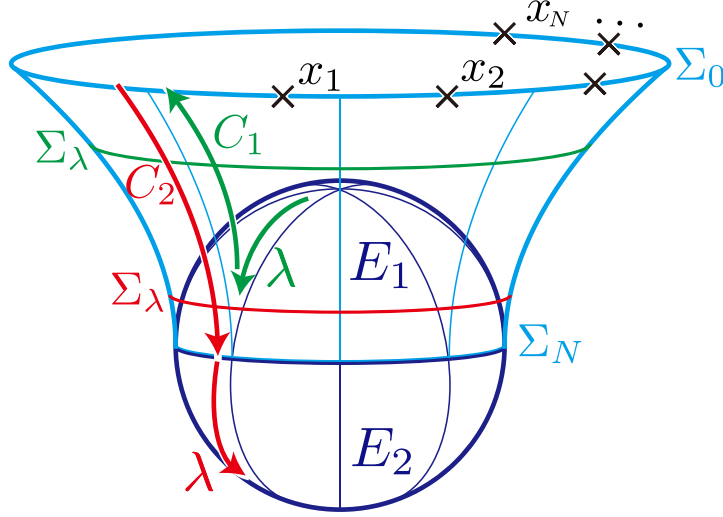


**Figure 3.** A 4-dimensional CDL instanton embedded in 5-dimensional Minkowski spacetime. The integral that gives an  $N$ -point correlation function on a spatial hypersurface  $\Sigma_0$  (eq. (4.2)) is performed along a path,  $\lambda$ , and over space,  $\mathbf{x}$ . The  $\lambda$  integration is done along  $C = C_1 + C_2$ , and the  $\mathbf{x}$  integration is done over a hypersurface  $\Sigma_\lambda$  for a given  $\lambda$ . The upper cylinder (light blue) is the Lorentzian region after bubble nucleation. The upper and lower hemispheres (dark blue) are the Euclidean regions  $E_1$  and  $E_2$ , respectively. A bubble is assumed to be nucleated on the hypersurface  $\Sigma_N$ . (The bubble wall is not shown.) The hypersurfaces  $\Sigma_\lambda$  are chosen to be Cauchy surfaces in the Lorentzian region, and are chosen to cover  $E_1$  and  $E_2$  in the Euclidean regions of the integration domain  $V_1$  (the green arrows ending on  $\Sigma_0$ ) and  $V_2$  (the red arrows ending in  $E_2$ ), respectively.

To evaluate eq. (4.2), we use Wick's theorem after Taylor expanding the exponential. Due to the path-ordering operator,  $P$ , each pair of field operators becomes  $G_P(x, x')$ , which is given by

$$G_P(x, x') \equiv \langle 0 | P \varphi(x) \varphi(x') | 0 \rangle = \begin{cases} G^+(x, x') & \text{when } x' \text{ precedes } x \\ G^-(x, x') & \text{when } x \text{ precedes } x' \end{cases}, \quad (4.3)$$

where  $G^\pm(x, x')$  are the Wightman functions given by eq. (3.15).

Let us briefly comment on analyticity of  $G_P(x, x')$  (see appendix B for details). This function is singular when  $x$  and  $x'$  are null-separated. However, by assuming a small imaginary part in the time coordinates along the in-in path in eq. (4.2),  $G_P(x, x')$  becomes analytical. As a result,  $\langle \varphi(x_1) \varphi(x_2) \cdots \varphi(x_N) \rangle$  is also analytical with respect to  $x_i$ s.

## 5 Bispectrum from open inflation

### 5.1 Cubic action in the flat gauge

To calculate the bispectrum at the tree-level, we substitute the constraint equations into the original action, keep  $O(\varphi^3)$  quantities, and obtain the reduced third-order action in the flat gauge (in which  $\zeta \equiv 0$ ).

The third-order action to the leading order in the slow-roll parameters is  $O(\epsilon^{1/2})$  and given by (see appendix A.2 for derivation)

$$\begin{aligned}
S_3 = & - \int dt d^3\mathbf{x} \sqrt{\gamma} a^5 \dot{\phi} [(\partial^2 - 3)^{-1} \dot{\phi}] \dot{\phi}^2 \\
& + \int dt d^3\mathbf{x} \sqrt{\gamma} \left\{ a^5 \ddot{\phi} [(\partial^2 - 3)^{-1} \dot{\phi}] \dot{\phi}^2 + \frac{3a^3 \dot{\phi}}{4H} [(\partial^2 - 3)^{-1} \dot{\phi}] \left( \dot{\phi}^2 + \frac{1}{a^2} \partial_i \varphi \partial^i \varphi \right) \right\} \\
& + \int dt d^3\mathbf{x} \left\{ -\frac{a^2 \dot{\phi}}{4H} \left[ (\partial^2 - 3)^{-1} \left( \dot{\phi}^2 + \frac{1}{a^2} \partial_i \varphi \partial^i \varphi \right) \right] - \frac{a^2}{2H} [(\partial^2 - 3)^{-1} \dot{\phi}] (\dot{\phi} \dot{\phi} - \ddot{\phi} \varphi) \right\} \frac{\delta \mathcal{L}}{\delta \varphi},
\end{aligned} \tag{5.1}$$

where  $\delta \mathcal{L}/\delta \varphi \equiv a^3 \sqrt{\gamma} \delta L/\delta \varphi$ , with  $\delta L/\delta \varphi$  given in eq. (3.11), and  $\partial^2 \equiv \gamma^{ij} \partial_i \partial_j$ . Let us check the correspondence between this action and that found by Clunan and Seery [31], who give the third-order action with positive spatial curvature.

- We need to replace their  $\partial^2 + 3$  (denoted as  $\Delta + 3$ ) with  $\partial^2 - 3$ , as we deal with negative curvature.
- The first line in eq. (5.1) agrees with the second term in their eq. (4.5).
- The second line in eq. (5.1) does not appear in their action: the first term proportional to  $\ddot{\phi}$  is ignored in their action because it is a higher order in slow-roll in their model. While  $\ddot{\phi}/(H\dot{\phi})$  is slow-roll suppressed in the usual inflation scenario, it is not so in open inflation because  $\ddot{\phi}/(H\dot{\phi}) = \mathcal{O}(1)$  soon after bubble nucleation. The second term proportional to  $3a^3 \dot{\phi}/(4H)$  does not appear in their action due to the difference in EOM. Had our EOM had an extra mass term like theirs, the second term would cancel out with a term in the second line.
- The last line of eq. (5.1) agrees with the last term in their eq. (4.5) with  $f(\varphi)$  given in their eq. (4.6), except for the sign of the second term in their eq. (4.6). This is because their second-order action (eq. (2.15)) contains an extra mass term of  $V'' = -3/a^2$ .
- The first term in their eq. (4.5),  $(aH/\dot{\phi})\varphi^3$ , which comes from  $V'''$ , is ignored in our action.

As in the case of the second order action, we expect that this expression derived in the  $R$ -region can also be used outside the  $R$ -region by analytical continuation, except near the bubble wall, for which a non-zero mass term should be inserted into the action. Potentially large self-interaction terms near the bubble wall do not contribute to the bispectrum in the sub-curvature approximation, as discussed in appendix C.

The terms in the second line are proportional to the EOM; thus, we remove it by making the field redefinition [44],  $\varphi \rightarrow \varphi_c$ , where

$$\varphi = \varphi_c + \frac{\dot{\phi}}{4H} [(\partial^2 - 3)^{-1} \partial_i \varphi_c \partial^i \varphi_c] + \dots, \tag{5.2}$$

where  $\dots$  contains terms which vanish outside the horizon. The field redefinition does not affect the second-order action,  $S_2$ , given in eq. (3.3). The positive-frequency function for  $\varphi_c$  is given by eqs. (3.13) with (3.14).

We write the interaction Lagrangian density,  $\mathcal{L}_{int}$ , in terms of  $\varphi_c$  as

$$\begin{aligned} \mathcal{L}_{int} = \sqrt{\gamma} \Big\{ & -a^5 \dot{\phi} [(\partial^2 - 3)^{-1} \dot{\phi}_c] \dot{\phi}_c^2 + a^5 \ddot{\phi} [(\partial^2 - 3)^{-1} \varphi_c] \dot{\phi}_c^2 \\ & + \frac{3a^3 \dot{\phi}}{4H} [(\partial^2 - 3)^{-1} \varphi_c] \left( \dot{\phi}_c^2 + \frac{1}{a^2} \partial_i \varphi_c \partial^i \varphi_c \right) \Big\}. \end{aligned} \quad (5.3)$$

If we write eq. (5.2) schematically as  $\varphi = \varphi_c + \lambda \varphi_c^2$ , the 3-point function of  $\varphi$  is given by

$$\begin{aligned} \langle \varphi(x_1) \varphi(x_2) \varphi(x_3) \rangle = & \langle \varphi_c(x_1) \varphi_c(x_2) \varphi_c(x_3) \rangle \\ & + \lambda \left[ \langle \varphi_c(x_1) \varphi_c(x_2) \rangle \langle \varphi_c(x_1) \varphi_c(x_3) \rangle + (\text{perms.}) \right], \end{aligned} \quad (5.4)$$

where  $\langle \varphi_c(x_1) \varphi_c(x_2) \varphi_c(x_3) \rangle$  is obtained by substituting  $\mathcal{L}_{int}$  (eq. (5.3)) into the expression for the  $N$ -point function given in eq. (4.2).

## 5.2 An example calculation

Before we compute the bispectrum using the cubic action given by eq. (5.3), let us show how the calculation proceeds using a simpler example. Consider  $\mathcal{L}_{int}$  given by

$$\mathcal{L}_{int}(x) = \sqrt{-g} \lambda_{int}(t) \varphi^3(x). \quad (5.5)$$

Although  $\mathcal{L}_{int}(x)$  that we wish to use is not in this form, both eqs. (5.3) and (5.5) respect  $O(4)$ -symmetry of the background universe; thus, the calculations proceed essentially in the same way.

Using eq. (4.2), Wick's theorem, and eq. (4.3), we obtain the tree-level 3-point function for space-like separated points  $x_1$ ,  $x_2$ , and  $x_3$  as

$$\langle \varphi(x_1) \varphi(x_2) \varphi(x_3) \rangle = 2\text{Re} \left[ -i \int_{V_2} d^4x \sqrt{-g} \lambda_{int}(t) G^+(x, x_1) G^+(x, x_2) G^+(x, x_3) \right] + (\text{perms.}), \quad (5.6)$$

As the direct evaluation of the real-space expression such as eq. (5.6) is often not practical, we shall move to the harmonic-space expression by operating  $\prod_{i=1}^3 \int d^3\mathbf{x}_i \sqrt{\gamma} Y_{p_i l_i m_i}^*(\mathbf{x}_i)$  on both sides of eq. (5.6), and using eqs. (3.15), (3.13), (3.7), and (3.16). We shall only consider the modes with  $p^2 > 0$ . Orthogonality of  $Y_{p_i l_i m_i}$  then implies that super-curvature modes with  $p^2 < 0$  do not contribute.

As a result of  $O(4)$ -symmetry of the system, the harmonic-space expression always contains a geometrical factor given by  $\int d^3\mathbf{x} \sqrt{\gamma} Y_{p_1 l_1 m_1}(\mathbf{x}) Y_{p_2 l_2 m_2}(\mathbf{x}) Y_{p_3 l_3 m_3}(\mathbf{x}) = \mathcal{F}_{p_1 p_2 p_3}^{l_1 l_2 l_3} \mathcal{G}_{l_1 l_2 l_3}^{m_1 m_2 m_3}$ , where

$$\mathcal{F}_{p_1 p_2 p_3}^{l_1 l_2 l_3} \equiv \int dr \sinh^2 r f_{p_1 l_1}(r) f_{p_2 l_2}(r) f_{p_3 l_3}(r), \quad (5.7)$$

$$\mathcal{G}_{l_1 l_2 l_3}^{m_1 m_2 m_3} \equiv \int d^2\Omega Y_{l_1 m_1}(\Omega) Y_{l_2 m_2}(\Omega) Y_{l_3 m_3}(\Omega). \quad (5.8)$$

See appendix B for the issue on the integration outside the  $R$ -region in  $V_2$  in eq. (5.6). The bispectrum,  $B(p_1, p_2, p_3)$ , is given by

$$\langle \varphi_{p_1 l_1 m_1} \varphi_{p_2 l_2 m_2} \varphi_{p_3 l_3 m_3} \rangle = B(p_1, p_2, p_3) \mathcal{F}_{p_1 p_2 p_3}^{l_1 l_2 l_3} \mathcal{G}_{l_1 l_2 l_3}^{m_1 m_2 m_3}. \quad (5.9)$$



As we show in appendix C, the contribution to the bispectrum in the sub-curvature approximation ( $p \gg 1$ ) mainly comes from the  $R$ -region, and the bispectrum at late time (i.e.,  $\eta \approx 0$ ) is given by

$$B(p_1, p_2, p_3) \approx 2\text{Re} \left\{ -iv_{p_1}(0)v_{p_2}(0)v_{p_3}(0) \left[ \int_{-\infty}^0 a^4(\eta) d\eta \lambda_{int}(\eta) u_{p_1}(\eta) u_{p_2}(\eta) u_{p_3}(\eta) \right] + (\text{perms.}) \right\}. \quad (5.10)$$

The contribution from outside the  $R$ -region can be included by extending the integration domain to the complex plane (see eq. (B.9) in appendix B). Whilst eq. (5.10) was obtained from  $\mathcal{L}_{int}$  given in eq. (5.5),  $B(p_1, p_2, p_3)$  calculated from the true  $\mathcal{L}_{int}$  given in eq. (5.3) takes a similar form.

### 5.3 Bispectrum in the sub-curvature approximation

In this section we calculate the bispectrum from open inflation in the sub-curvature approximation,  $p \gg 1$ . This approximation is justified because we have not yet detected spatial curvature within our current horizon. As we show in appendix D, the power spectrum,  $P(p)$ , and the bispectrum,  $B(p_1, p_2, p_3)$ , reduce to  $P(k)$  and  $B(k_1, k_2, k_3)$  in the sub-curvature approximation with  $p_i \rightarrow k_i$ , where  $k_i$ 's denote Fourier wavenumbers defined in flat space. Therefore, we shall use  $k_i$  for the indices of harmonics instead of  $p_i$ .

We calculate the bispectrum using the same method as was used to derive eq. (5.10), but replacing  $\mathcal{L}_{int}$  in eq. (5.5) with that given in eq. (5.3).

#### 5.3.1 Bispectrum of $\varphi$

First, let us compute the bispectrum from the field redefinition term. Recalling  $P(k) = H_I^2/(2k^3)$  in the sub-curvature approximation, we find

$$B^{(\text{redef})}(k_1, k_2, k_3) = \frac{\dot{\phi}}{4H_I} \frac{\mathbf{k}_1 \cdot \mathbf{k}_2}{k_3^2 + 4} \frac{H_I^2}{2k_1^3} \frac{H_I^2}{2k_2^3} + (\text{perms.}). \quad (5.11)$$

Second, we compute the bispectrum from the in-in integral. As we show in appendix C, the leading-order term in the sub-curvature approximation is the first term in eq. (5.3),

$$\mathcal{L}_{int}^{(1)} \equiv -\sqrt{\gamma} a^5 \dot{\phi} [(\partial^2 - 3)^{-1} \dot{\phi}_c] \dot{\phi}_c^2, \quad (5.12)$$

and the other terms are sub-dominant. We thus compute

$$B(k_1, k_2, k_3) = 2\text{Re} \left\{ iv_{k_1}(0)v_{k_2}(0)v_{k_3}(0) \left[ \int_{-\infty}^0 d\eta \frac{a^6 \dot{\phi}}{k_1^2 + 4} \dot{u}_{k_1}(\eta) \dot{u}_{k_2}(\eta) \dot{u}_{k_3}(\eta) \right] + (\text{perms.}) \right\}. \quad (5.13)$$

The mode functions,  $u_k(\eta)$ ,  $\dot{u}_k(\eta)$ , and  $v_k(0)$ , are given by (see eq. (3.14))

$$u_k(\eta) \approx \begin{cases} -\frac{i}{a(\eta)\sqrt{2k}} \left( e^{-ik\eta} - e^{-\pi k - 2i\delta_k} e^{ik\eta} \right) & (-\infty < \eta \lesssim -1) \\ \frac{H_I}{\sqrt{2k^3}} \left[ (1 + ik\eta) e^{-ik\eta} - e^{-\pi k - 2i\delta_k} (1 - ik\eta) e^{ik\eta} \right] & (-1 \lesssim \eta < 0) \end{cases}, \quad (5.14)$$

$$\dot{u}_k(\eta) \approx \frac{1}{a^2(\eta)} \sqrt{\frac{k}{2}} \left( e^{-ik\eta} + e^{-\pi k - 2i\delta_k} e^{ik\eta} \right), \quad (5.15)$$

$$v_k(0) = u_k^*(0) \approx \frac{H_I}{\sqrt{2k^3}} (1 - e^{-\pi k - 2i\delta_k}), \quad (5.16)$$

where we have kept the terms proportional to  $e^{-\pi k} e^{ik\eta}$ , despite that they are suppressed by  $e^{-\pi k}$ . This is because these terms represent the effect of a non-Bunch-Davies initial state, and we shall discuss the effect of these terms toward the end of this subsection.

Ignoring the non-Bunch-Davies terms for the moment, we obtain

$$B(k_1, k_2, k_3) = 2\text{Re} \left[ i \left( 2 \sum_{i=1}^3 \frac{H_I^3}{k_i^2} \right) \frac{1}{8k_1 k_2 k_3} \int_{-\infty}^0 d\eta \dot{\phi} e^{-i(k_1+k_2+k_3)\eta} \right]. \quad (5.17)$$

Using eq. (2.21) for  $\dot{\phi}$ , the integration during the curvature-dominated era (i.e.,  $-\infty < \eta < -1$ ) is given by

$$\int_{-\infty}^{-1} d\eta \dot{\phi} e^{-i(k_1+k_2+k_3)\eta} = -\frac{3\sqrt{2\epsilon}H_I}{2} \frac{e^{-1+i(k_1+k_2+k_3)}}{1-i(k_1+k_2+k_3)}, \quad (5.18)$$

and that during the inflationary era (i.e.,  $-1 < \eta < 0$ ) is given by

$$\int_{-1}^0 d\eta \dot{\phi} e^{-i(k_1+k_2+k_3)\eta} = -\sqrt{2\epsilon}H_I \frac{1-e^{i(k_1+k_2+k_3)}}{-i(k_1+k_2+k_3)}. \quad (5.19)$$

We thus find, in  $k \gg 1$ ,

$$B(k_1, k_2, k_3) = \frac{\sqrt{2\epsilon}H_I^4}{4k_1 k_2 k_3 (k_1 + k_2 + k_3)} \left( \sum_{i=1}^3 \frac{1}{k_i^2} \right) \left[ 2 - 0.9 \cos(k_1 + k_2 + k_3) \right], \quad (5.20)$$

where the factor 0.9 comes from  $-2 + 3e^{-1} \approx -0.9$ . This result is based upon the approximate form for  $\dot{\phi}$  given in eq. (2.21), which is discontinuous at  $\eta = -1$ . We find that the second oscillatory term in eq. (5.20) is an artifact due to this discontinuity.<sup>7</sup> To show this, we use the numerical solution of eq. (2.17) for  $\dot{\phi}$  and evaluate the integral. In figure 4, we show that the numerical solution does not contain any oscillations. Henceforth we shall neglect the oscillatory terms coming from the discontinuity of the approximate solution of  $\dot{\phi}$ . We obtain

$$B(k_1, k_2, k_3) = \frac{2\sqrt{2\epsilon}H_I^4}{4k_1 k_2 k_3 (k_1 + k_2 + k_3)} \left( \sum_{i=1}^3 \frac{1}{k_i^2} \right), \quad (5.21)$$

which agrees with the result for the single-field slow-roll inflation models with the canonical kinetic term [44]. In the squeezed limit,  $k_3 \ll k_1 \approx k_2 \equiv k$ , we find

$$B(k_1, k_2, k_3) \rightarrow \frac{\sqrt{2\epsilon}H_I^4}{4k^3 k_3^3} = \sqrt{2\epsilon}P(k)P(k_3). \quad (5.22)$$

The bispectrum from the field redefinition term (eq. (5.11)) in the squeezed limit goes as

$$B^{(\text{redef})}(k_1, k_2, k_3) \rightarrow -\frac{\sqrt{2\epsilon}H_I^4}{16} \frac{1}{k^4 k_3^2} = -\sqrt{2\epsilon} \frac{k_3}{4k} P(k)P(k_3). \quad (5.23)$$

Thus, the field redefinition term is sub-dominant in this limit.

Next, let us discuss an enhancement of the bispectrum due to a non-Bunch-Davies vacuum initial state,  $B^{(\text{NBD})}(k_1, k_2, k_3)$ . The relevant term in eq. (5.15) is the part of  $\dot{u}_k(\eta)$

---

<sup>7</sup>We would like to thank T. Tanaka for pointing this out.

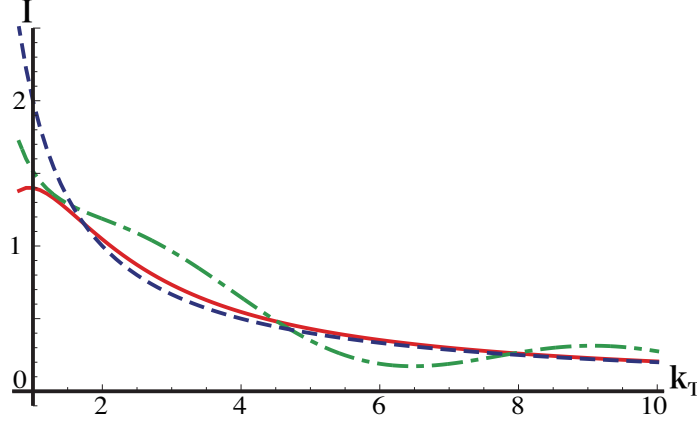


**Figure 4.** We calculate the integral given by  $I \equiv (1/2\sqrt{\epsilon}H_I)2\text{Re}[i \int_{-\infty}^0 d\eta \dot{\phi} e^{-ik_T\eta}]$  with  $k_T \equiv k_1 + k_2 + k_3$  in three ways. First, we use the numerical solution of eq. (2.17) for  $\dot{\phi}$  in the integral [solid (red) line]. Second, we use the approximate solution for  $\dot{\phi}$  given in (2.21) [dot-dashed (green) line]. This gives the term in the square bracket in eq. (5.20) divided by  $k_T$ . Finally, we remove the oscillatory term from the second case [dashed (blue) line]. This result is in good agreement with the full solution (solid line) for sub-curvature modes ( $1 \ll k_T$ ), justifying our ignoring the oscillatory term in eq. (5.21) and thereafter.

that is proportional to  $e^{ik\eta}$  (i.e.,  $\dot{v}_k(\eta)$ ) instead of  $e^{-ik\eta}$  (i.e.,  $\dot{u}_k(\eta)$ ). We then do this flipping in each of  $\dot{u}_{k_i}$  in the integral of eq. (5.13). For example, flipping  $\dot{u}_{k_1}$  we obtain

$$\begin{aligned}
& B^{(\tilde{v}_{k_1})}(k_1, k_2, k_3) \\
&= 2\text{Re} \left[ i \left( 2 \sum_{i=1}^3 \frac{H_I^3}{k_i^2} \right) \frac{e^{-\pi k_1 - 2i\delta_{k_1}}}{4k_1 k_2 k_3} \int_{-\infty}^0 d\eta \dot{\phi} e^{-i(-k_1 + k_2 + k_3)\eta} \right] \\
&= \frac{\sqrt{2\epsilon}H_I^4 e^{-\pi k_1}}{8k_1 k_2 k_3} \left( \sum_{i=1}^3 \frac{1}{k_i^2} \right) \text{Re} \left[ e^{-2i\delta_{k_1}} \left( 2 \frac{1 - e^{i(-k_1 + k_2 + k_3)}}{-k_1 + k_2 + k_3} - 3i \frac{e^{-1 + i(-k_1 + k_2 + k_3)}}{1 - i(-k_1 + k_2 + k_3)} \right) \right].
\end{aligned} \tag{5.24}$$

Flipping  $\dot{u}_{k_2}$  or  $\dot{u}_{k_3}$  will similarly give  $B^{(\tilde{v}_{k_2})}$  or  $B^{(\tilde{v}_{k_3})}$ ; hence  $B^{(\text{NBD})} = \sum_{i=1}^3 B^{(\tilde{v}_{k_i})}$  to the leading order of  $e^{-\pi k}$ . We are interested in a peculiar behavior of the bispectrum from a non-Bunch-Davies initial state in the squeezed limit,  $k_3 \ll k_1 \approx k_2 \equiv k$  [38–40], while still satisfying the sub-curvature approximation,  $1 \ll |-k_1 + k_2 + k_3|$ . Again ignoring the oscillatory term which is an artifact of using the approximate form of  $\dot{\phi}$  in eq. (2.21), we find

$$\begin{aligned}
B^{(\text{NBD})}(k_1, k_2, k_3) &\rightarrow 2\sqrt{\frac{\epsilon}{2}}H_I^4 \cos(2\delta_k) \frac{e^{-\pi k}}{k_3^4 k^2} \\
&= 4\sqrt{2\epsilon} \cos(2\delta_k) e^{-\pi k} \frac{k}{k_3} P(k) P(k_3).
\end{aligned} \tag{5.25}$$

There is an enhancement factor in the squeezed limit,  $k/k_3 \gg 1$ , compared to the usual single-field model with a Bunch-Davies initial state,  $B(k, k, k_3) \propto k_3^{-3} k^3$  (see eq. (5.22)). This result is in agreement with the previous work on the effect of modified initial states

on the bispectrum, in which modifications are given by hand [38–40]. Despite the enhancement factor by  $k/k_3$ , however,  $B^{(\text{NBD})}(k_1, k_2, k_3)$  is always subdominant in the sub-curvature approximation due to the exponential suppression factor,  $e^{-\pi k}$ .

Let us now consider the exact folded limit,  $k_i = k_j + k_l$ . In the previous study on the effect of modified initial states (given by hand) on the bispectrum, the bispectrum diverges in this limit [35–37]. However, a self-consistent computation presented here gives a finite result. There is one subtlety: in order for us to use Fourier wavenumbers defined in flat space,  $k_i$ , we need to make sure that  $k_i + k_j - k_l$  for any combinations of  $i, j$ , and  $k$  are greater than unity (i.e., sub-curvature approximation). This requirement is not met in the exact folded limit. We thus go back to the open harmonics with  $p_i$ . Also taking the squeezed limit,  $p_3 \ll p_1 \approx p_2 \equiv p$ , for simplicity, we obtain a compact formula,

$$B^{(\text{NBD})}(p, p - p_3, p_3) \rightarrow -3.1 \sqrt{\frac{\epsilon}{2}} H_I^4 \sin(2\delta_p) \frac{e^{-\pi p}}{p_3^3 p^2}, \quad (5.26)$$

which remains finite, and is suppressed by  $e^{-\pi p}$ .

### 5.3.2 Bispectrum of $\zeta$

To compute the late-time observables such as the temperature and polarization anisotropy of the CMB, we need to compute the curvature perturbation on a uniform-density hypersurface,  $\zeta$ , which is equal to a “comoving” ( $\varphi = 0$ ) hypersurface and is conserved outside the horizon. We thus perform the following non-linear transformation relating the scalar-field fluctuation in the flat gauge,  $\varphi$ , to  $\zeta$  [65] (also see eq. (2.66) of ref. [66])

$$\begin{aligned} \zeta &= \int_{\phi_* + \varphi_*}^{\phi_*} d\phi \frac{H}{\dot{\phi}} \\ &= -\frac{H_*}{\dot{\phi}_*} \varphi_* - \frac{1}{2} \frac{\partial}{\partial \phi} \left( \frac{H}{\dot{\phi}} \right) \Big|_{\phi=\phi_*} \varphi_*^2 + \mathcal{O}(\varphi_*^3) \\ &= -\frac{H_*}{\dot{\phi}_*} \varphi_* + \frac{1}{2} \left( \frac{H_* \ddot{\phi}_*}{\dot{\phi}_*^3} + \frac{1}{2} \right) \varphi_*^2 + \mathcal{O}(\varphi_*^3), \end{aligned} \quad (5.27)$$

where the subscript  $*$  indicates the moment of the horizon exit, and  $H_* \approx H_I$  during slow-roll inflation. The first term in eq. (5.27) implies that the bispectrum of  $\varphi$  computed in the previous section times  $-H_*^3/\dot{\phi}_*^3$  yields the bispectrum of  $\zeta$ . In addition, the second-term yields an additional contribution to the bispectrum of  $\zeta$ .

In the sub-curvature approximation, the power spectrum of  $\varphi$  given in eq. (3.17) multiplied by  $H_*^2/\dot{\phi}_*^2 = 1/(2\epsilon_*)$  with  $p \rightarrow k$  yields

$$P_\zeta(k) = \frac{H_*^2}{4\epsilon_*} \frac{1}{k^3}. \quad (5.28)$$

Using the relation  $k = a_* H_*$  and taking into account the slow-roll time-dependence of  $H_*$  and  $\epsilon_*$ , we obtain the power spectrum index as

$$n_s - 1 \equiv \frac{d \ln k^3 P_\zeta(k)}{d \ln k} = -2 \frac{\ddot{\phi}_*}{H_* \dot{\phi}_*} - 2 \frac{\dot{\phi}_*^2}{H_*^2}. \quad (5.29)$$

Ignoring the non-Bunch-Davies terms and taking the squeezed limit,  $k_3 \ll k_1 \approx k_2 \equiv k$ , we obtain from eqs. (5.22) and (5.27)

$$\begin{aligned} B_\zeta(k_1, k_2, k_3) &\rightarrow -\frac{H_I^3}{\dot{\phi}_*^3} \frac{H_I^4 \sqrt{2\epsilon_*}}{4k^3 k_3^3} + \frac{2H_I^2}{\dot{\phi}_*^2} \left( \frac{H_I \ddot{\phi}_*}{\dot{\phi}_*^3} + \frac{1}{2} \right) \frac{H_I^2}{2k_3^3} \frac{H_I^2}{2k^3} \\ &= (1 - n_s) P_\zeta(k) P_\zeta(k_3), \end{aligned} \quad (5.30)$$

where we have used  $\sqrt{2\epsilon_*} = -\dot{\phi}_*/H_I$  (recall  $\dot{\phi} < 0$  during slow-roll inflation in our model). This result agrees with the squeezed limit of the usual single-field inflation models with a Bunch-Davies initial state [44]. Therefore, aside from the terms suppressed in the sub-curvature approximation, Maldacena’s consistency relation,  $B_\zeta \rightarrow (1 - n_s) P_\zeta(k) P_\zeta(k_3)$  as  $k_3 \rightarrow 0$ , holds. However, note that we are not taking the *exact* squeezed limit,  $k_3 \rightarrow 0$ ; rather, we are working in the sub-curvature approximation, and thus  $k_3$  has to satisfy  $k_3 \gg 1$ . Also, once again, eq. (5.30) is valid at the leading order in the sub-curvature approximation. See appendix C for sub-leading contributions.

## 6 Conclusion

In this paper, we have computed the bispectrum from a single-field open inflation model, in which a single scalar field is responsible for both quantum tunneling (nucleation of a bubble inside of which we live) and slow-roll inflation inside a bubble after tunneling. We assume that the potential energy inside the bubble at the onset of slow-roll inflation is approximately equal to the false vacuum energy density of the background de Sitter space.

A comoving observer in de Sitter space charted by open coordinates detects particles with respect to the Euclidean vacuum state (which is equivalent to the Bunch-Davies vacuum state in de Sitter space charted by flat coordinates), in the same sense that a comoving observer in Minkowski space charted by Rindler coordinates detects particles with respect to the Minkowski vacuum state. Moreover, quantum tunneling modifies an initial state for quantum fluctuations away from the Euclidean vacuum state. Therefore, open inflation naturally provides a “non-Bunch-Davies” initial state for quantum fluctuations. The occupation number of particles detected inside the bubble has a thermal spectrum, exponentially falling off at large momenta.

Most of the previous work on the effect of modified initial states for quantum fluctuations puts mode functions characterizing a non-Bunch-Davies initial state by hand at an artificial initial time. Instead of doing this, we compute the effect of a non-Bunch-Davies vacuum on the bispectrum self-consistently within the framework of open inflation. An “initial time” naturally emerges because slow-roll inflation follows the period of a curvature-dominated era right after quantum tunneling. The mode functions (hence the initial state) are uniquely fixed given a model of open inflation.

We find that the bispectrum of the curvature perturbation on a uniform-density hypersurface,  $\zeta$ , has a term going as  $B_\zeta(k, k, k_3) \propto e^{-\pi k} k_3^{-4} k^{-2}$  in the squeezed limit,  $k_3 \ll k_1 \approx k_2 \equiv k$ . (The units are such that  $k \approx 1$  is a wavenumber corresponding to the curvature radius of our universe.) This bispectrum rises more sharply toward small  $k_3$  than that of the standard single-field inflation model,  $B_\zeta(k, k, k_3) \propto k_3^{-3} k^{-3}$ , by a factor of  $k/k_3 \gg 1$ . This behaviour agrees with phenomenological studies done by the previous work [38–40]. However, the amplitude of the bispectrum is exponentially suppressed by  $e^{-\pi k}$  in the sub-curvature region,  $k \gg 1$ , i.e., for wavelengths shorter than the present-day curvature radius. Given that

we do not see evidence for spatial curvature within our current horizon, we conclude that the non-Bunch-Davies effect of open inflation on the observable bispectrum is exponentially suppressed. This is a consequence of the occupation number of particles detected in our bubble falling off exponentially at large momenta. We also find that the bispectrum in the exact folded limit, e.g.,  $k_1 = k_2 + k_3$ , remains finite.

The leading-order bispectrum from open inflation in the sub-curvature approximation is similar to that of the standard single-field model with a Bunch-Davies initial state. The bispectrum specific for open inflation arises only in the sub-leading order in the sub-curvature approximation, which is suppressed at least by the factor  $1/k_i$  ( $\ll 1$ ) compared to the leading-order bispectrum.

Open inflation provides an attractive framework within which we can discuss the origin of *our* universe without its initial singularity. It is thus worthwhile to find any observable signatures of open inflation. We have shown that the bispectrum picks up some signatures of open inflation, although they are exponentially suppressed in the model we have explored. On the other hand, it is possible that the false vacuum energy density is much greater than the potential energy inside the bubble. In such a case, the high false vacuum energy may overcome the exponential suppression factor,  $e^{-\pi k}$ . Also, while we have ignored the effect of super-curvature modes (for which  $p^2 < 0$  where  $p$  is the wavenumber of the open harmonics), they may become important when the false vacuum energy density is high [34].

## Acknowledgments

KS would like to thank J. White, D. Yamauchi, T. Tanaka and M. Sasaki for useful discussions and valuable comments. KS would also like to thank Max-Planck-Institut für Astrophysik for hospitality, where this work was initiated and completed. This work was supported in part by Monbukagakaku-sho Grant-in-Aid for the Global COE programs, “The Next Generation of Physics, Spun from Universality and Emergence” at Kyoto University. KS was supported by Grant-in-Aid for JSPS Fellows No. 23-3437.

## A Expansion of action in a FLRW universe with negative spatial curvature

In this appendix, we derive the reduced action for scalar-type perturbations by perturbatively expanding the full action, which consists of the Einstein-Hilbert action, the York-Gibbons-Hawking term, and the scalar-field action. With the metric given in eq. (3.2), the full action is given by

$$S = \frac{1}{2} \int dt d^3 \mathbf{x} \sqrt{h} \left\{ N \left[ R^{(3)} - 2V - h^{ij} \partial_i \phi(t, \mathbf{x}) \partial_j \phi(t, \mathbf{x}) \right] + \frac{1}{N} \left( E_{ij} E^{ij} - E^2 + \left[ \dot{\phi}(t, \mathbf{x}) - N^i \partial_i \phi(t, \mathbf{x}) \right]^2 \right) \right\}, \quad (\text{A.1})$$

where

$$E_{ij} \equiv \frac{1}{2} \left( \dot{h}_{ij} - \partial_i N_j - \partial_j N_i \right), \quad E = h^{ij} E_{ij}, \quad (\text{A.2})$$

and  $R^{(3)}$  is the 3-dimensional Ricci scalar.

In an open FLRW universe, where the curvature of the universe is given by  $K = -1$ , the action has a similar form as in the case of a closed FLRW universe with  $K = 1$ , which has

been studied by Clunan and Seery [31]. However, there is one big difference. In open inflation, where  $\dot{\phi}(t) = 0$  and  $H(t) \equiv \dot{a}(t)/a(t) = \infty$  at the initial time,  $t = 0$ ,  $\epsilon(\equiv (dV/d\phi)^2/(2V^2)) \ll 1$  guarantees  $\dot{\phi}^2/(2H^2) \ll 1$  at all times. In a closed universe, where  $H(t) = 0$  at the time of bounce,  $\dot{\phi}^2/(2H^2) \ll 1$  is not satisfied for  $\epsilon \ll 1$ . ref. [31] thus imposes a different condition on  $V(\phi)$  in order to satisfy  $\dot{\phi}^2/(2H^2) \ll 1$ .

### A.1 Second-order action

As in section 3, taking the uniform curvature (flat) gauge ( $\zeta = 0$ ), we expand  $\phi$  around the uniform background,  $\phi(t)$ , as  $\phi(t, \mathbf{x}) = \phi(t) + \varphi(t, \mathbf{x})$ , and hereafter denote  $\phi(t)$  as  $\phi$ . We obtain the reduced action by solving the constraint equations after gauge fixing. For the second- or third-order action, it is enough to solve the constraint equations up to  $O(\varphi)$  [44].

By writing  $N = 1 + \delta N$  and  $N^i = \gamma^{ij} \partial_j \chi$ , we obtain the Hamiltonian constraint and the momentum constraint up to  $O(\varphi)$ , respectively, as

$$2\frac{dV}{d\phi}\varphi + 2\delta N(-6H^2 + \dot{\phi}^2) - 4H\partial^2\chi - 2\dot{\phi}\dot{\varphi} = 0, \quad (\text{A.3})$$

$$\partial_i \left[ 2H\delta N - 2K\chi - \dot{\phi}\dot{\varphi} \right] = 0. \quad (\text{A.4})$$

From these equations, we obtain  $\delta N$  and  $\chi$  up to  $O(\varphi)$ , respectively, as

$$\delta N = \frac{\dot{\phi}}{2H}\varphi + \frac{K}{H}\chi, \quad (\text{A.5})$$

$$\chi \approx -\frac{1}{2H}(\partial^2 + 3K)^{-1} \left( \dot{\phi}\dot{\varphi} - \ddot{\phi}\varphi \right). \quad (\text{A.6})$$

Here, we have kept only the leading-order terms in the expansion in  $\dot{\phi}^2/(2H^2)$  in eq. (A.6). This expansion is equivalent to the expansion in the slow-roll parameter,  $\epsilon$ . Both  $\delta N$  and  $\chi$  are  $O(\epsilon^{1/2})$  quantities. We keep the term proportional to  $\ddot{\phi}$  in eq. (A.6), as  $\ddot{\phi}/(H\dot{\phi})$  is an  $O(1)$  quantity in the curvature-dominated era. It is however slow-roll suppressed during the slow-roll inflationary era.

By substituting eqs. (A.5) and (A.6) into eq. (A.1) and keeping quantities up to  $O(\varphi^2)$ , we obtain the second-order action as

$$\begin{aligned} S_2 = \int dt d^3\mathbf{x} a^3 \sqrt{\gamma} & \left[ \left( -\frac{(d^2V/d\phi^2)}{2} - \frac{\dot{\phi}(dV/d\phi)}{2H} \right) \varphi^2 + \frac{1}{2a^2} \partial_i \varphi \partial^i \varphi + K \partial_i \chi \partial^i \chi + \frac{1}{2} \dot{\varphi}^2 \right. \\ & \left. - \frac{\dot{\phi}^2}{H} \varphi \dot{\varphi} - \frac{K(dV/d\phi)}{H} \chi \varphi - \frac{K\dot{\phi}}{H} \chi \dot{\varphi} + \left( -3 + \frac{\dot{\phi}^2}{2H^2} \right) \left( \frac{\dot{\phi}^2}{4} \varphi^2 + K \dot{\phi} \chi \varphi + \chi^2 \right) \right] \\ & \approx \int dt d^3\mathbf{x} a^3 \sqrt{\gamma} \left[ \frac{1}{2} \dot{\varphi}^2 - \frac{1}{2a^2} \partial_i \varphi \partial^i \varphi \right], \end{aligned} \quad (\text{A.7})$$

where the sub-leading terms in the slow-roll expansion are neglected in the last expression. This is eq. (3.3) in section 2.

### A.2 Third-order action

We also keep only the leading-order quantities in the slow-roll expansion in the third-order action. By substituting eqs. (A.5) and (A.6) into eq. (A.1) and keeping quantities up to



$O(\varphi^3)$ , we obtain

$$S_3 = \int dt d^3 \mathbf{x} \sqrt{\gamma} \left[ - \left( \frac{a^3 \dot{\phi} \varphi}{4H} + \frac{K a^3 \chi}{2H} \right) \left( \dot{\varphi}^2 + \frac{1}{a^2} \partial_i \varphi \partial^i \varphi \right) - a^3 \dot{\varphi} \partial_i \chi \partial^i \varphi \right], \quad (\text{A.8})$$

where  $S_3$  is an  $O(\epsilon^{1/2})$  quantity.

The last term in eq. (A.8) can be integrated by parts to give

$$- \int dt d^3 \mathbf{x} \sqrt{\gamma} a^3 \dot{\varphi} \partial_i \chi \partial^i \varphi = \int dt d^3 \mathbf{x} \sqrt{\gamma} \left( -\frac{3}{2} a^3 H \chi \partial_i \varphi \partial^i \varphi - \frac{1}{2} a^3 \dot{\chi} \partial_i \varphi \partial^i \varphi + a^3 \chi \dot{\varphi} \partial^2 \varphi \right). \quad (\text{A.9})$$

The last term in this expression can be integrated by parts again to give

$$\int dt d^3 \mathbf{x} \sqrt{\gamma} a^3 \chi \dot{\varphi} \partial^2 \varphi = \int dt d^3 \mathbf{x} \left\{ \left[ \sqrt{\gamma} \left( \frac{a^5 H}{2} \chi \dot{\varphi}^2 - \frac{a^5}{2} \dot{\chi} \dot{\varphi}^2 \right) \right] + a^2 \chi \dot{\varphi} \frac{\delta \mathcal{L}}{\delta \varphi} \right\}, \quad (\text{A.10})$$

where the Lagrangian density,  $\mathcal{L}$ , is defined by the second-order action as  $S_2 = \int d^4 x \mathcal{L}$ . Substituting this back into eq. (A.9) we get

$$- \int dt d^3 \mathbf{x} \sqrt{\gamma} a^3 \dot{\varphi} \partial_i \chi \partial^i \varphi = \int dt d^3 \mathbf{x} \left\{ \left[ \sqrt{\gamma} \left( \frac{a^5 H}{2} \chi (\dot{\varphi}^2 - 3 \partial_i \varphi \partial^i \varphi) - \frac{a^5}{2} \dot{\chi} \left( \dot{\varphi}^2 + \frac{1}{a^2} \partial_i \varphi \partial^i \varphi \right) \right) \right] + a^2 \chi \dot{\varphi} \frac{\delta \mathcal{L}}{\delta \varphi} \right\}. \quad (\text{A.11})$$

The time derivative of  $\chi$  can be written as

$$\dot{\chi} = -\frac{K}{a^2 H} \chi - 3H\chi - \frac{\dot{\phi}}{2Ha^2} \varphi + \frac{3K\dot{\phi}}{2Ha^2} (\partial^2 + 3K)^{-1} \varphi + \frac{\dot{\phi}}{2H} (\partial^2 + 3K)^{-1} \frac{\delta L}{\delta \varphi}, \quad (\text{A.12})$$

where  $\delta L/\delta \varphi$  is given in eq. (3.11). ( $L$  is related to  $\mathcal{L}$  by  $\mathcal{L} = a^3 \sqrt{\gamma} L$ .) We have ignored the term proportional to  $\ddot{\phi}$  using  $|\ddot{\phi}/(H^2 \dot{\phi})| \ll 1$ , which can be derived from eq. (2.21). By substituting eq. (A.12) into eq. (A.11), we obtain

$$\begin{aligned} & - \int dt d^3 \mathbf{x} \sqrt{\gamma} a^3 \dot{\varphi} \partial_i \chi \partial^i \varphi \\ &= \int dt d^3 \mathbf{x} \left\{ \left[ \sqrt{\gamma} \left( 2a^5 H \chi \dot{\varphi}^2 + \left( \frac{K a^3 \chi}{2H} + \frac{a^3 \dot{\phi}}{4H} \varphi - \frac{3K a^3 \dot{\phi}}{4H} (\partial^2 + 3K)^{-1} \varphi \right) \left( \dot{\varphi}^2 + \frac{1}{a^2} \partial_i \varphi \partial^i \varphi \right) \right) \right] \right. \\ & \quad \left. + \left( -\frac{a^2 \dot{\phi}}{4H} \left( \dot{\varphi}^2 + \frac{1}{a^2} \partial_i \varphi \partial^i \varphi \right) (\partial^2 + 3K)^{-1} + a^2 \chi \dot{\varphi} \right) \frac{\delta \mathcal{L}}{\delta \varphi} \right\}. \end{aligned} \quad (\text{A.13})$$

Finally, substituting eq. (A.13) into eq. (A.8), we obtain the third-order action

$$\begin{aligned} S_3 &= \int dt d^3 \mathbf{x} \sqrt{\gamma} \left[ -a^5 (\partial^2 + 3K)^{-1} (\dot{\phi} \dot{\varphi} - \ddot{\phi} \varphi) \dot{\varphi}^2 - \frac{3K a^3 \dot{\phi}}{4H} (\partial^2 + 3K)^{-1} \varphi \left( \dot{\varphi}^2 + \frac{1}{a^2} \partial_i \varphi \partial^i \varphi \right) \right] \\ & \quad + \int dt d^3 \mathbf{x} \left[ -\frac{a^2 \dot{\phi}}{4H} \left( \dot{\varphi}^2 + \frac{1}{a^2} \partial_i \varphi \partial^i \varphi \right) (\partial^2 + 3K)^{-1} - \frac{a^2}{2H} (\partial^2 + 3K)^{-1} \dot{\varphi} (\dot{\phi} \dot{\varphi} - \ddot{\phi} \varphi) \right] \frac{\delta \mathcal{L}}{\delta \varphi}. \end{aligned} \quad (\text{A.14})$$

This is eq. (5.1) in section 5 after moving  $(\partial^2 + 3K)^{-1}$  in the first term in the second line to the left by integration by parts, and replacing  $K$  with  $K = -1$ .

## B Analytical structure of the universe in open inflation

### B.1 Coordinate systems and Wightman functions

The coordinate system defined by eqs. (2.6) to (2.9) is suitable for studying one of the mode functions forming a complete set,  $u_{\mathbf{k}}(x)$ , which multiplies the annihilation operator,  $\hat{a}_{\mathbf{k}}$ , in eq. (3.4). Let us call this coordinate system “ $K_2$ .” The  $K_2$  is suitable for  $u_{\mathbf{k}}(x)$  because the  $R$ -,  $L$ - and  $C$ -regions are connected via  $E_2$ , and  $u_{\mathbf{k}}(x)$  is analytical in and across all the regions.

On the other hand,  $K_2$  is *not* suitable for studying another mode function,  $v_{\mathbf{k}}(x)$ , which multiplies the creation operator,  $\hat{a}_{\mathbf{k}}^\dagger$ , in eq. (3.4). We thus introduce a new set of coordinate systems, which we shall call “ $K_1$ .” The  $K_1$  is defined by

$$\begin{aligned} \begin{cases} \tau & (-\pi/(2H_I) \leq \tau \leq \pi/(2H_I)) \\ \chi & (0 \leq \chi \leq \pi) \end{cases}, & \begin{cases} t_R = -i(\tau - \pi/(2H_I)) & (0 \leq t_R < \infty) \\ r_R = i(\chi - \pi) & (0 \leq r_R < \infty), \end{cases} \\ \begin{cases} t_L = -i(-\tau - \pi/(2H_I)) & (0 \leq t_L < \infty) \\ r_L = i(\chi - \pi) & (0 \leq r_L < \infty), \end{cases}, & \begin{cases} t_C = \tau & (-\pi/(2H_I) \leq t_C \leq \pi/(2H_I)) \\ r_C = i(\chi - \pi/2) & (0 \leq r_C < \infty), \end{cases} \end{aligned} \quad (\text{B.1})$$

with the coordinates of a 2-sphere  $\Omega^i$  commonly used for all regions. For simplicity, we assume that the spacetime is approximately de Sitter with the metric given by eq. (2.10). In the  $K_1$  system, the  $R$ -,  $L$ - and  $C$ -regions are connected via  $E_1$ , and  $v_{\mathbf{k}}(x)$  is analytical in and across all the regions. The difference between  $K_2$  and  $K_1$  is not a mere coordinate transformation, but they define the relations between the  $E$ -,  $R$ -,  $L$ -, and  $C$ -regions in a different way.

The two Wightman functions coincide for space-like separated  $x$  and  $x'$ , i.e.,  $G^+(x, x') = G^-(x, x') \equiv G(x, x')$ , where  $G^+(x, x') = \sum_{\mathbf{k}} u_{\mathbf{k}}(x) v_{\mathbf{k}}(x')$  and  $G^-(x, x') = \sum_{\mathbf{k}} u_{\mathbf{k}}(x') v_{\mathbf{k}}(x)$ ; however, they are different for time-like separated  $x$  and  $x'$ . The Wightman functions diverge when  $x$  is on the past- or future-light cones of  $x'$ . This divergence is the so-called UV divergence of the Wightman functions.

In performing calculations it is necessary to choose one of the two sets of coordinate systems,  $K_2$  or  $K_1$ , and to choose one of the two Wightman functions,  $G^+(x, x')$  or  $G^-(x, x')$ . We shall discuss the origin of these possible options, in terms of the analytical structure of de Sitter space charted by these coordinates. We shall then explain as to why  $u_{\mathbf{k}}(x)$  is analytical in  $K_2$ , whilst  $v_{\mathbf{k}}(x)$  is not; and why  $v_{\mathbf{k}}(x)$  is analytical in  $K_1$ , whilst  $u_{\mathbf{k}}(x)$  is not [18].

To discuss the analytical structure of de Sitter space charted by these coordinates, let us chart the 5-dimensional Minkowski spacetime,  $ds_5^2 = \eta_{ab} dx^a dx^b$  with  $\eta = \text{diag}(-1, 1, 1, 1, 1)$ , by the Cartesian coordinates

$$x = (x^0, x^1, x^2, x^3, x^4). \quad (\text{B.2})$$

The 4-dimensional de Sitter spacetime is embedded as a hyperboloid defined by

$$-(x^0)^2 + \sum_{i=1}^4 (x^i)^2 = \frac{1}{H_I^2}. \quad (\text{B.3})$$

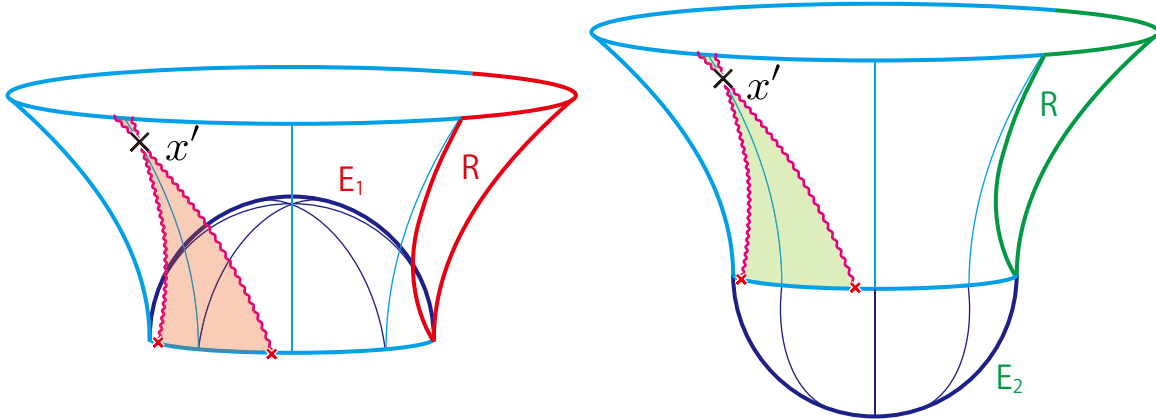


**Figure 5.** Analytical continuation. (Left) The  $R$ -region is connected to the  $C$ -region via  $E_1$  by  $x^+$ , where  $\text{Im } x^0 > 0$ . (Right) The  $R$ -region is connected to the  $C$ -region via  $E_2$  by  $x^-$ , where  $\text{Im } x^0 < 0$ . The Wightman function,  $G(x, x')$ , is uniquely determined in the space-like region of  $x'$ , but it diverges on the light-cone of  $x'$  shown by the wavy lines. Analytically extending  $G(x, x')$  into the past-light cone of  $x'$  using  $x^+$  and  $x^-$ , we obtain  $G^-(x, x')$  in the shaded area in the left panel and  $G^+(x, x')$  in the shaded area in the right panel, respectively.

The Euclidean region is given by imposing  $x^0$  to be pure imaginary, and it is related to the coordinates given in eqs. (2.6) to (2.9) or eq. (B.1) as [51]

$$ix^0 = \cos \tau \cos \chi, \quad x^1 = \sin \tau, \quad \begin{pmatrix} x^2 \\ x^3 \\ x^4 \end{pmatrix} = \cos \tau \sin \chi \mathbf{\Omega}, \quad (\text{B.4})$$

where  $\mathbf{\Omega} = (\Omega^1, \Omega^2, \Omega^3)$  is a 3-dimensional unit vector. With the Cartesian coordinates, we can discuss the analytical structure of de Sitter spacetime without worrying about coordinate singularities.

In QFT on an open inflation background, we encounter two types of singularities. One is a coordinate singularity and the other is a UV divergence of the Wightman functions. The first issue is the coordinate singularity. Let us consider the coordinates  $(t_C, r_C, \Omega)$  defined in the  $C$ -region (i.e.,  $(-\pi/(2H_I) \leq t_C \leq \pi/(2H_I))$  and  $0 \leq r_C < \infty$ ) with the metric given by the fourth line of eq. (2.10). The coordinates in the  $C$ -region are analytical<sup>8</sup> (i.e., the metric is analytical and non-singular), which means that even if the coordinates are given only in a finite part of the  $C$ -region, we can analytically extend them to the whole  $C$ -region. However, coordinate singularities appear on the boundaries between the  $C$ - and  $R$ -regions and the  $C$ - and  $L$ -regions, and the analytical extension of the coordinate system beyond these boundaries seems not possible, even though the spacetime is extended.

The second issue is the UV divergence of the Wightman functions. Let us fix  $x'$  and regard the Wightman function,  $G(x, x')$ , as a function of  $x$ . As  $G(x, x')$  is analytical in the space-like region of  $x'$ , we can analytically extend it to the whole space-like region of  $x'$ , even if  $G(x, x')$  is given only in a finite part of the space-like region of  $x'$ . However,  $G(x, x')$  diverges on the past- or future-light cones of  $x'$ , and again, the analytical extension of  $G(x, x')$  beyond the past- or future-light cones of  $x'$  seems not possible.

<sup>8</sup>There is no difference between  $K_1$  and  $K_2$  in the  $C$ -region.

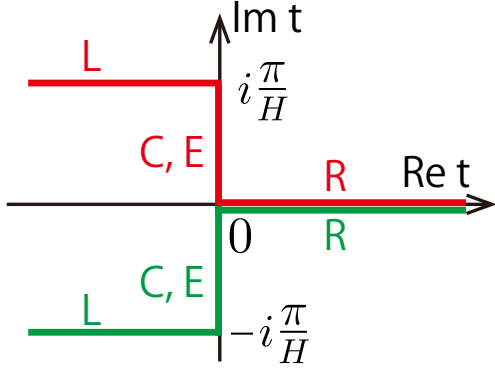


**Figure 6.** Correspondence between the domains of  $t$  and the  $E$ -,  $R$ -,  $L$ -, and  $C$ -regions. The upper (red) lines show the integration path  $V_1$  charted by  $K_1$ , while the bottom (green) lines show  $V_2$  charted by  $K_2$ .

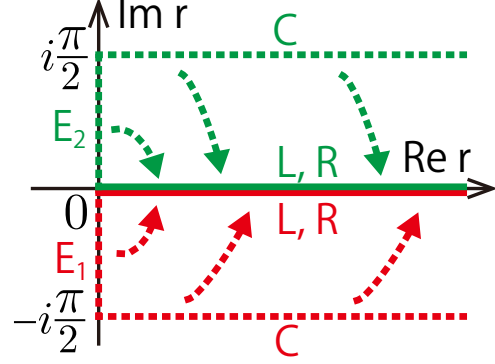


**Figure 7.** Same as figure 6, but for  $r$ . The bottom (red) dashed lines show the original integration path  $V_1$  charted by  $K_1$ , while the upper (green) dashed lines show  $V_2$  charted by  $K_2$ . The integral can be evaluated by deforming the paths to lie along the real axis of  $r$ , as shown by the solid lines.

Those apparent issues regarding the analytical extension of the coordinates and the Wightman functions can be overcome by taking a path through the complex plane. By adding an infinitely small complex number,  $\pm i\epsilon$  ( $\epsilon > 0$ ), to  $x^0$ , we obtain

$$x^\pm = (x^0 \pm i\epsilon, x^1, x^2, x^3, x^4). \quad (\text{B.5})$$

Since  $x^\pm$  no longer passes right through the singularities, the coordinates and the Wightman functions can be analytically extended to all the regions charted by  $K_1$  or  $K_2$ .

Let us take  $x^+$  first, and see how the analytical extension is performed. The coordinate system defined in the  $C$ -region can be analytically extended with  $x^+$  beyond the coordinate singularities on the boundaries between the  $C$ - and  $R$ -regions and the  $C$ - and  $L$ -regions. As  $\text{Im } x^0 > 0$  in  $E_1$ , the resulting set of coordinate systems corresponds to  $K_1$ , which connects the  $R$ -,  $L$ -, and  $C$ -regions via  $E_1$  (see figure 5). The Wightman function  $G(x, x')$ , considered as a function of  $x$  for a given  $x'$  ( $x$  is in the space-like region of  $x'$ ), can be analytically extended by shifting  $x^+$  beyond the past-light cone of  $x'$ , where  $G(x, x')$  diverges (see section 5.4 of ref. [53]). As a result,  $G^-(x, x')$  is obtained inside the past-light cone of  $x'$  as shown in figure 5. Since the analyticity of  $v_{\mathbf{k}}(x)$  and  $G^-(x, x')$  with respect to  $x$  are equivalent, the analyticity of  $v_{\mathbf{k}}(x)$  with respect to  $x^+$  is also guaranteed, which leads to the analyticity of  $v_{\mathbf{k}}(x)$  with respect to  $K_1$  and the regularity of  $v_{\mathbf{k}}(x)$  on  $E_1$ .

Similarly, the analytical extension using  $x^-$  gives  $K_2$ , which connects the  $R$ -,  $L$ -, and  $C$ -regions via  $E_2$ . As a result,  $G^+(x, x')$  is obtained inside the past-light cone of  $x'$ . Then  $u_{\mathbf{k}}(x)$  is analytical with respect to  $K_2$  and is regular on  $E_2$ .

## B.2 Deformation of integration path using analyticity

Thanks to the analyticity of  $u_{\mathbf{k}}(x)$  and  $v_{\mathbf{k}}(x)$  with respect to the set of coordinate systems  $K_2$  and  $K_1$ , respectively, we can deform the path of integration given in eq. (4.2). For

simplicity, we shall consider the tree-level calculation and write the integral schematically as  $\int_{(C_1+C_2)\times\Sigma_\lambda} d\lambda d^3\mathbf{x} \sqrt{-g} f(x)$ .

Let us consider the integral over  $V_1 = C_1 \times \Sigma_\lambda$  in the coordinate system  $K_1$ . We can use the coordinates in the  $R$ -region,  $t$  and  $r$ , in the whole  $V_1$  by allowing  $t$  and  $r$  to be complex variables. Using the relation between coordinates given by eq. (B.1),  $V_1$  is given by the sum of

$$\begin{aligned} E_1 &= \{(t, r, \Omega) | t \in (0, i\pi/H_I), r \in (0, -i\pi/2), \Omega \in S_2\} , \\ C &= \{(t, r, \Omega) | t \in (0, i\pi/H_I), r \in (-i\pi/2, -i\pi/2 + \infty), \Omega \in S_2\} , \\ R &= \{(t, r, \Omega) | t \in (0, \infty), r \in (0, \infty), \Omega \in S_2\} , \\ L &= \{(t, r, \Omega) | t \in (i\pi/H_I, -\infty), r \in (0, \infty), \Omega \in S_2\} , \end{aligned} \quad (\text{B.6})$$

where, for simplicity, we additionally assume that  $\Sigma_0$  is in the far future of the nucleation surface and that the Lorentzian region of  $V_1$  can be approximated as the whole de Sitter spacetime after the nucleation time. We can then simplify the integration domain by deforming the integration path as

$$\int_{C_1 \times \Sigma_\lambda} d\lambda d^3\mathbf{x} \sqrt{-g} f(x) = \int_{i\pi/H_I - \infty}^{\infty} dt \int_0^{\infty} dr \int d\Omega \sqrt{-g} f(x). \quad (\text{B.7})$$

The upper (red) lines in figure 6 show the integration path along  $t$ , while the bottom (red) lines in figure 7 show how we deform the integration path to lie along the real axis of  $r$ . The deformation shown in figure 7 is possible because the integrand  $\sqrt{-g} f(x)$  (which is a function of the background quantities and  $v_{\mathbf{k}}(x)$ , both of which are analytical) is analytical with respect to  $t$  and  $r$  given by eq. (B.6), and  $\sqrt{-g} f(x)$  falls off rapidly as  $\text{Re } r \rightarrow \infty$  for sub-curvature modes, i.e.,  $p^2 > 0$  for which the open harmonics falls off as  $f_{pl}(r) \propto e^{-r}$  (see eq. (3.6)). However, this deformation would not be valid for super-curvature modes, which we ignore in this paper.

Similarly, with the set of coordinate systems  $K_2$  given by eqs. (2.6) to (2.9), the domain of integration  $V_2 = C_2 \times \Sigma_\lambda$  is given by the sum of

$$\begin{aligned} E_2 &= \{(t, r, \Omega) | t \in (0, -i\pi/H_I), r \in (0, i\pi/2), \Omega \in S_2\} , \\ C &= \{(t, r, \Omega) | t \in (0, -i\pi/H_I), r \in (i\pi/2, i\pi/2 + \infty), \Omega \in S_2\} , \\ R &= \{(t, r, \Omega) | t \in (0, \infty), r \in (0, \infty), \Omega \in S_2\} , \\ L &= \{(t, r, \Omega) | t \in (-i\pi/H_I, -\infty), r \in (0, \infty), \Omega \in S_2\} , \end{aligned} \quad (\text{B.8})$$

and we can simplify the integration domain by deforming the integration path as

$$\int_{C_2 \times \Sigma_\lambda} d\lambda d^3\mathbf{x} \sqrt{-g} f(x) = - \int_{-i\pi/H_I - \infty}^{\infty} dt \int_0^{\infty} dr \int d\Omega \sqrt{-g} f(x), \quad (\text{B.9})$$

as is shown in the bottom (green) lines in figure 6 and the upper (green) lines in figure 7.

In the single-field open inflation model that we study in this paper, the mode functions contributing to the bispectrum in the  $R$ -region vanish outside the bubble. Thus, eqs. (B.7) and (B.9) further simplify to

$$\int_{C_1 \times \Sigma_\lambda} d\lambda d^3\mathbf{x} \sqrt{-g} f(x) = \int_{iR_W}^{\infty} dt \int_0^{\infty} dr \int d\Omega \sqrt{-g} f(x), \quad (\text{B.10})$$

$$\int_{C_2 \times \Sigma_\lambda} d\lambda d^3\mathbf{x} \sqrt{-g} f(x) = - \int_{-iR_W}^{\infty} dt \int_0^{\infty} dr \int d\Omega \sqrt{-g} f(x), \quad (\text{B.11})$$

respectively, where  $R_W$  is the bubble radius measured in the coordinates of the  $E$ -regions.

## C Order-of-magnitude estimate for sub-leading contributions

In section 5.3, we have computed the leading-order contribution to the bispectrum,  $\mathcal{L}_{int}^{(1)}$ , in the  $R$ -region, but have ignored the other contributions. In this appendix, we show that the contributions from the other terms in  $\mathcal{L}_{int}$  are sub-dominant in the sub-curvature approximation. We also show that the contributions from outside the  $R$ -region are sub-dominant in the sub-curvature approximation, which implies that the effects of possibly large self-interaction near the bubble wall are also sub-dominant. For simplicity, we shall show the result only in the squeezed configuration,  $k_3 \ll k_1 \approx k_2 (\equiv k)$ .

In the following calculations, we change the integration variable from  $t$  to the conformal time,  $\eta$ , in the integration given in eq. (B.11). Accordingly, the integration domain changes from  $t : -iR_W \rightarrow 0 \rightarrow \infty$  to  $\eta : \eta_W \rightarrow -\infty \rightarrow 0$ , where  $\eta_W$  is given by

$$\eta_W \equiv -\frac{1}{2} \log \left( \frac{\cosh H_I t + 1}{\cosh H_I t - 1} \right) \Bigg|_{t=-iR_W} \quad \left( \Leftrightarrow \quad e^{\eta_W} = \left( \frac{H_I R_W}{\sqrt{2}} \right) e^{-i\pi/2} \right). \quad (\text{C.1})$$

The approximate forms of  $a$ ,  $H$ ,  $\dot{\phi}$ ,  $\ddot{\phi}$ , and  $u_k$  given in eqs. (2.20), (2.21), and (5.14) originally obtained with the condition  $-\infty < \eta \lesssim -1$  can also be used when  $\eta \in (\eta_W, -\infty)$ . This is because the approximate forms for  $-\infty < \eta \lesssim -1$  (or  $0 < t \lesssim H_I^{-1}$ ) are obtained using  $|tH_I| \ll 1$ , which is also satisfied for  $\eta \in (\eta_W, -\infty)$  (or  $t \in (-iR_W, 0)$ ), as the radius of the nucleated bubble is smaller than the Hubble scale (i.e.,  $H_I R_W \lesssim 1$ ). Throughout this appendix, we shall ignore the effects of the non Bunch-Davies vacuum state, as we show in section 5.3 that these effects are sub-dominant in the sub-curvature approximation.

### C.1 Contributions from outside the $R$ -region

We calculate the contribution to the leading-order bispectrum,  $B^{(1)}(k_1, k_2, k_3)$ , from  $\mathcal{L}_{int}^{(1)}$  outside the  $R$ -region,  $\eta \in (\eta_W, -\infty)$ . Using the same methods as were used to obtain eq. (5.17),  $B^{(1)}(k_1, k_2, k_3)$  is given by

$$B^{(1)}(k_1, k_2, k_3) = 2\text{Re} \left[ i v_{k_1}(0) v_{k_2}(0) v_{k_3}(0) \left( \int_{\eta_W}^{-\infty} d\eta \frac{a^6 \dot{\phi}}{k_1^2 + 4} \dot{u}_{k_1}(\eta) \dot{u}_{k_2}(\eta) \dot{u}_{k_3}(\eta) \right) + (\text{perms.}) \right], \quad (\text{C.2})$$

where only the integration domain is different from eq. (5.17). Substituting eqs. (2.21), (5.14), (5.15), and (C.1) into eq. (C.2), we obtain

$$\begin{aligned} B^{(1)}(k_1, k_2, k_3) &= 2\text{Re} \left[ i \left( \frac{H_I^3}{k_1^2} \right) \frac{1}{8k_1 k_2 k_3} \int_{\eta_W}^{-\infty} d\eta \dot{\phi} e^{-i(k_1+k_2+k_3)\eta} + (\text{perms.}) \right] \\ &\approx \frac{\sqrt{\epsilon} H_I^4 e^{-\pi(2k+k_3)/2}}{k_3^3 k^3} H_I R_W, \end{aligned} \quad (\text{C.3})$$

where we do not show an  $O(1)$  pre-factor, which does not affect the order-of-magnitude estimate.

The exponential suppression factor,  $e^{-\pi(2k+k_3)/2}$ , appears because the mode functions of sub-curvature modes are exponentially suppressed outside the  $R$ -region. (One may check this by substituting  $\eta \in (\eta_W, -\infty)$  into  $u_k(\eta)$  given in eq. (3.9).) This factor makes eq. (C.3) much smaller than  $B(k_1, k_2, k_3)$  in eq. (5.21) in the sub-curvature approximation. This suppression

is universal for any integrations outside the  $R$ -region. We thus conclude that the integration of all terms in  $\mathcal{L}_{int}$  outside the  $R$ -region is negligible in the sub-curvature approximation. This also implies that the contribution from the possibly large self-interaction near the bubble wall (which is in the  $C$ - and  $E$ -regions) is negligible in the sub-curvature approximation.

## C.2 Contributions from the sub-leading terms in Lagrangian

Next, we calculate the contributions from the other terms of  $\mathcal{L}_{int}$  given in eq. (5.3). In addition to the leading-order term,  $\mathcal{L}_{int}^{(1)}$ , there are three terms:

$$\begin{aligned}\mathcal{L}_{int}^{(2)} &= \sqrt{\gamma} a^5 \ddot{\phi} (\partial^2 - 3)^{-1} \varphi_c \dot{\phi}_c^2, \\ \mathcal{L}_{int}^{(3)} &= \sqrt{\gamma} \frac{3a^3 \dot{\phi}}{4H} (\partial^2 - 3)^{-1} \varphi_c \dot{\phi}_c^2, \\ \mathcal{L}_{int}^{(4)} &= -\sqrt{\gamma} \frac{3a^3 \dot{\phi}}{4H} (\partial^2 - 3)^{-1} \varphi_c \frac{1}{a^2} \partial_i \varphi_c \partial^i \varphi_c.\end{aligned}\tag{C.4}$$

As the integral outside the  $R$ -region is negligible in the sub-curvature approximation, we shall consider the contributions from the integral inside the  $R$ -region.

Let us start with  $\mathcal{L}_{int}^{(2)}$ . The relative size of  $\mathcal{L}_{int}^{(2)}$  compared to  $\mathcal{L}_{int}^{(1)}$  is  $\mathcal{L}_{int}^{(2)}/\mathcal{L}_{int}^{(1)} \approx \ddot{\phi} \varphi_c / \dot{\phi} \dot{\phi}_c$ . According to eqs. (2.21), (5.14), and (5.15), this ratio is  $\ddot{\phi} \varphi_c / \dot{\phi} \dot{\phi}_c \approx aH/k$  for  $-\infty < \eta \lesssim -1$ , and  $\ddot{\phi} \varphi_c / \dot{\phi} \dot{\phi}_c \approx O(\epsilon)$  for  $-1 \lesssim \eta < 0$ . The ratio in  $-1 \lesssim \eta < 0$  is slow-roll suppressed. The ratio in  $-\infty < \eta \lesssim -1$  is small for sub-horizon modes with  $k/(aH) \gg 1$ . The horizon size and the curvature radius are comparable, i.e.,  $aH \approx 1$ , during the curvature-dominated era,  $-\infty < \eta \lesssim -1$ . Therefore, the ratio in  $-\infty < \eta \lesssim -1$  is suppressed in the sub-curvature approximation,  $k \gg 1$ .

Next, we calculate the contribution from  $\mathcal{L}_{int}^{(3)}$ . The bispectrum is

$$\begin{aligned}B^{(3)}(k_1, k_2, k_3) &= 2\text{Re} \left[ i u_{k_1}(0) u_{k_2}(0) u_{k_3}(0) \left( \int_{-\infty}^0 d\eta \frac{a^4 \dot{\phi}}{4H(\eta)(k_1^2 + 4)} u_{k_1}(\eta) \dot{u}_{k_2}(\eta) \dot{u}_{k_3}(\eta) \right) \right. \\ &\quad \left. + (\text{perms.}) \right].\end{aligned}\tag{C.5}$$

Using eqs. (2.20), (2.21), (5.14), and (5.15), we estimate the contribution from  $\eta \in (-1, 0)$  as

$$\sqrt{\epsilon} H^4 \text{Re} \left[ i \frac{1}{k_1^5 k_2 k_3} \int_{-1}^0 d\eta (1 + ik_1 \eta) e^{-i(k_1 + k_2 + k_3)\eta} \right] + (\text{perms.}) \approx \frac{\sqrt{\epsilon} H^4}{k_3^4 k^3},\tag{C.6}$$

where the integral is estimated as  $O(k_1/k_T)$  with  $k_T \equiv k_1 + k_2 + k_3$ . Using eqs. (2.20), (2.21), (5.14), and (5.15), we estimate the contribution from  $\eta \in (-\infty, -1)$  as

$$\frac{\sqrt{\epsilon} H^4}{k_1^4 k_2 k_3} \text{Re} \left[ \int_{-\infty}^{-1} d\eta e^{\eta} e^{-ik_1 \eta} e^{-ik_2 \eta} e^{-ik_3 \eta} \right] + (\text{perms.}) \approx \frac{\sqrt{\epsilon} H^4}{k_3^4 k^3},\tag{C.7}$$

where the integral is estimated as  $O(k_T^{-1})$ . We thus find

$$B^{(3)}(k_1, k_2, k_3) \approx \frac{\sqrt{\epsilon} H^4}{k_3^4 k^3},\tag{C.8}$$

up to a factor of  $\mathcal{O}(1)$ . This term is negligible compared to the leading term given in eq. (5.21) in the sub-curvature approximation,  $k_3 \gg 1$ .



Finally, we calculate the contribution from  $\mathcal{L}_{int}^{(4)}$ . The bispectrum is

$$\begin{aligned}
& B^{(4)}(k_1, k_2, k_3) \\
&= 2\text{Re} \left[ i u_{k_1}(0) u_{k_2}(0) u_{k_3}(0) \left( \int_{-\infty}^0 d\eta \frac{a^2 \dot{\phi}(-k_1^2 + k_2^2 + k_3^2 + 1)}{8H(\eta)(k_1^2 + 4)} u_{k_1}(\eta) u_{k_2}(\eta) u_{k_3}(\eta) \right) \right. \\
&\quad \left. + (\text{perms.}) \right], \tag{C.9}
\end{aligned}$$

where we have used the property of open harmonics

$$\int d^3\mathbf{x} \sqrt{\gamma} Y_{p_1 l_1 m_1} \partial_i Y_{p_2 l_2 m_2} \partial^i Y_{p_3 l_3 m_3} = \frac{-p_1^2 + p_2^2 + p_3^2 + 1}{2} \int d^3\mathbf{x} \sqrt{\gamma} Y_{p_1 l_1 m_1} Y_{p_2 l_2 m_2} Y_{p_3 l_3 m_3}. \tag{C.10}$$

Using eqs. (2.20), (2.21), and (5.14), we estimate the contribution from  $\eta \in (-1, 0)$  as

$$\begin{aligned}
& \frac{\sqrt{\epsilon} H^4 (-k_1^2 + k_2^2 + k_3^2)}{k_1^5 k_2^3 k_3^3} \text{Re} \left[ -i \int_{-1}^0 \frac{d\eta}{\eta^2} (1 + i k_1 \eta)(1 + i k_2 \eta)(1 + i k_3 \eta) e^{-i(k_1 + k_2 + k_3)\eta} \right] \\
& + (\text{perms.}) \approx \frac{\sqrt{\epsilon} H^4}{k_3^4 k^3}, \tag{C.11}
\end{aligned}$$

where the integral is estimated as  $O(k_1 k_2 k_3 / k_T)$ . Using eqs. (2.20), (2.21), and (5.14), we estimate the contribution from  $\eta \in (-\infty, -1)$  as

$$\frac{\sqrt{\epsilon} H^4 (-k_1^2 + k_2^2 + k_3^2)}{k_1^4 k_2^2 k_3^2} \text{Re} \left[ \int_{-\infty}^{-1} d\eta e^{\eta} e^{-i(k_1 + k_2 + k_3)\eta} \right] + (\text{perms.}) \approx \frac{\sqrt{\epsilon} H^4}{k_3^4 k^3}, \tag{C.12}$$

where the integral is estimated as  $O(k_T^{-1})$ . We thus find

$$B^{(4)}(k_1, k_2, k_3) \approx \frac{\sqrt{\epsilon} H^4}{k_3^4 k^3}, \tag{C.13}$$

up to a factor of  $\mathcal{O}(1)$ . This term is negligible compared to the leading term given in eq. (5.21) in the sub-curvature approximation,  $k_3 \gg 1$ .

## D Open harmonics in the sub-curvature approximation

### D.1 Correspondence with flat harmonics

In this appendix, we show the correspondence between the open and flat harmonics in the sub-curvature approximation, where the wavelength of the modes and the separation between points are assumed to be smaller than the curvature radius, i.e.,  $1 \ll p$  and  $r \ll 1$ , respectively.

On a 3-hyperboloid, whose spatial metric  $\gamma_{ij}$  is given by eq. (2.15), the open harmonics  $Y_{plm}(\mathbf{x})$  are defined by eq. (3.6). On a 3-dimensional flat space, whose metric is given by

$$\tilde{\gamma}_{ij} dx^i dx^j = dr^2 + r^2 d\Omega_2^2, \tag{D.1}$$

the flat spherical harmonics  $\tilde{Y}_{klm}(\mathbf{x})$  are defined by [67]

$$\tilde{Y}_{klm}(\mathbf{x}) = \Psi_{kl}(r) Y_{lm}(\Omega), \quad \Psi_{kl}(r) = \sqrt{\frac{2}{\pi}} k j_l(kr), \tag{D.2}$$

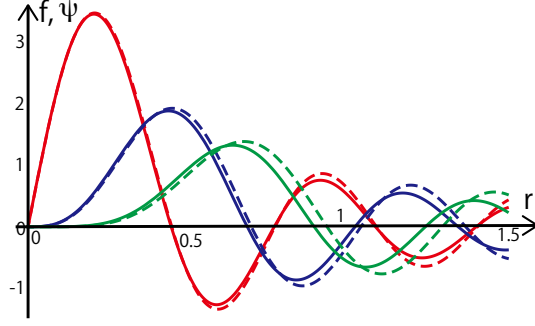


**Figure 8.** Comparison between  $f_{kl}(r)$  (solid lines) and  $\Psi_{kl}(r)$  (dashed lines) for  $l = 10$  as a function of  $r$ . The red, blue, and green lines show  $l = 1, 3$ , and  $5$ , respectively. The two functions agree well in  $r \ll 1$ .

where  $j_l(x)$  is the spherical Bessel function and  $Y_{lm}(\Omega)$  is the usual spherical harmonics on a 2-sphere. While  $Y_{plm}(\mathbf{x})$  satisfies the relations given by eq. (3.7),  $\tilde{Y}_{klm}(\mathbf{x})$  satisfies the following relations

$$\begin{aligned} \partial^2 \tilde{Y}_{klm}(\mathbf{x}) &= -k^2 \tilde{Y}_{klm}(\mathbf{x}), \\ \tilde{Y}_{klm}^*(\mathbf{x}) &= (-1)^m \tilde{Y}_{kl-m}(\mathbf{x}), \\ \int d^3\mathbf{x} \sqrt{\tilde{\gamma}} Y_{k_1 l_1 m_1}^*(\mathbf{x}) \tilde{Y}_{k_2 l_2 m_2}(\mathbf{x}) &= \delta(k_1 - k_2) \delta_{l_1 l_2} \delta_{m_1 m_2}, \\ \int_0^\infty dk \sum_{lm} \tilde{Y}_{klm}(\mathbf{x}) \tilde{Y}_{klm}(\mathbf{x}') &= \delta^{(3)}(\mathbf{x} - \mathbf{x}'). \end{aligned} \quad (\text{D.3})$$

To begin with, let us find the correspondence between  $Y_{plm}(\mathbf{x})$  and  $\tilde{Y}_{klm}(\mathbf{x})$ . As the angular parts  $Y_{lm}(\Omega)$  are the same for the open and flat harmonics, we focus on the correspondence between the radial parts, i.e.,  $f_{pl}(r)$  in eq. (3.6) and  $\Psi_{kl}(r)$  in eq. (D.2). The correspondence between  $f_{pl}(r)$  and  $\Psi_{kl}(r)$  with identification  $p \rightarrow k$  in the sub-curvature approximation,  $1 \ll p$  and  $r \ll 1$  is manifest in the differential equations that define the spherical Bessel functions and the associated Legendre functions in the sub-curvature approximation. In figure 8, we compare  $f_{pl}(r)$  (solid lines) and  $\Psi_{kl}(r)$  (dashed lines) as a function of  $r$  for  $p = k = 10$  and  $l = 1, 3$ , and  $5$ .

The asymptotic behaviours of these functions are useful for understanding their correspondence:

$$\Psi_{kl}(r) \rightarrow \begin{cases} \sqrt{\frac{2}{\pi}} \frac{\sin(kr - \frac{\pi}{2}l)}{k^{l+1} r^l} & (l \ll kr) \\ \frac{1}{2^{l+1/2} \Gamma(l + 3/2)} & (kr \ll l) \end{cases}, \quad (\text{D.4})$$

$$f_{pl}(r) \rightarrow \begin{cases} \sqrt{\frac{2}{\pi}} \frac{\sin(pr - \frac{\pi}{2}l)}{p^{l+1} r^l} & (l \ll pr, 1 \ll p) \\ \frac{1}{2^{l+1/2} \Gamma(l + 3/2)} & (pr \ll l, 1 \ll p) \end{cases}. \quad (\text{D.5})$$

In the sub-curvature approximation, where  $\sinh r \approx r$ ,  $f_{kl}(r)$  and  $\Psi_{kl}(r)$  agree with each other in the two opposite asymptotic regions,  $0 < r \ll l/k$  and  $l/k \ll r \ll 1$ .

Next, let us find the correspondence in the square and the cubic integrals of  $Y_{plm}(\mathbf{x})$  and  $\tilde{Y}_{klm}(\mathbf{x})$ . The correspondence in the square integrals is exact, as both of them form an orthonormal set. We write the cubic integrals for  $Y_{plm}(\mathbf{x})$  as

$$\int d^3\mathbf{x} \sqrt{\gamma} Y_{p_1 l_1 m_1}(\mathbf{x}) Y_{p_2 l_2 m_2}(\mathbf{x}) Y_{p_3 l_3 m_3}(\mathbf{x}) = \mathcal{F}_{p_1 p_2 p_3}^{l_1 l_2 l_3} \mathcal{G}_{l_1 l_2 l_3}^{m_1 m_2 m_3}, \quad (\text{D.6})$$

where  $\mathcal{F}_{k_1 k_2 k_3}^{l_1 l_2 l_3}$  is given in eq. (5.7) and  $\mathcal{G}_{l_1 l_2 l_3}^{m_1 m_2 m_3}$  is the Gaunt integral given in eq. (5.8). We write the cubic integrals for  $\tilde{Y}_{klm}(\mathbf{x})$  as

$$\int d^3\mathbf{x} \sqrt{\tilde{\gamma}} \tilde{Y}_{k_1 l_1 m_1}(\mathbf{x}) \tilde{Y}_{k_2 l_2 m_2}(\mathbf{x}) \tilde{Y}_{k_3 l_3 m_3}(\mathbf{x}) = \Psi_{k_1 k_2 k_3}^{l_1 l_2 l_3} \mathcal{G}_{l_1 l_2 l_3}^{m_1 m_2 m_3}, \quad (\text{D.7})$$

where  $\Psi_{k_1 k_2 k_3}^{l_1 l_2 l_3}$  is defined by

$$\Psi_{k_1 k_2 k_3}^{l_1 l_2 l_3} \equiv \int_0^\infty dr r^2 \Psi_{k_1 l_1}(r) \Psi_{k_2 l_2}(r) \Psi_{k_3 l_3}(r). \quad (\text{D.8})$$

As the angular parts are given by the Gaunt integral,  $\mathcal{G}_{m_1 m_2 m_3}^{l_1 l_2 l_3}$ , we shall focus on the correspondence between  $\mathcal{F}_{p_1 p_2 p_3}^{l_1 l_2 l_3}$  and  $\Psi_{k_1 k_2 k_3}^{l_1 l_2 l_3}$  with the identification of  $p_i \rightarrow k_i$  for all  $i = 1, 2$ , and 3 in the sub-curvature approximation,  $1 \ll p_i$ .

Strictly speaking, however,  $1 \ll p_i$  is not enough to show the correspondence in the cubic integral of harmonics. We thus additionally impose  $l_i \ll p_i$  for all  $i$  and  $1 \ll p_{\min}$  where  $p_{\min} \equiv \min(|\pm p_1 \pm p_2 \pm p_3|)$ . In the following, we shall use  $k$  not only for the indices of the flat harmonics, but also for those of the open harmonics.

Now, there exists an  $r^* (\ll 1)$  satisfying both  $1/k_{\min} \ll r^*$  where  $k_{\min} \equiv \min(|\pm k_1 \pm k_2 \pm k_3|)$  and  $l_i/k_i \ll r^*$  for all  $i$ . Using  $r^*$  we can divide the integral in eq. (D.8) into two parts, corresponding to  $0 < r < r^*$  and  $r^* < r < \infty$ . In the second part, by using the  $l \ll kr$  case of eq. (D.4) and the addition theorem for the sin functions, we can rewrite the integrand in the form of  $\sin[kr + (\text{phase})]/r$ , where  $k$  is one of  $\pm k_1 \pm k_2 \pm k_3$  for all combinations of  $\pm$ . Using the inequality

$$\begin{aligned} \left| \int_{r^*}^\infty \frac{\sin[kr + (\text{phase})]}{r} dr \right| &= \left| \left[ -\frac{\cos[kr + (\text{phase})]}{kr} \right]_{r^*}^\infty + \int_{r^*}^\infty \frac{\cos[kr + (\text{phase})]}{kr^2} dr \right| \\ &< \left| \frac{2}{kr^*} \right|, \end{aligned} \quad (\text{D.9})$$

and  $1 \ll k_{\min} r^*$ , we find that the integral over  $r^* < r < \infty$  is small and  $\Psi_{k_1 k_2 k_3}^{l_1 l_2 l_3}$  mainly comes from the integral over  $0 < r < r^*$ . Similarly, we find that  $\mathcal{F}_{k_1 k_2 k_3}^{l_1 l_2 l_3}$  mainly comes from the integral over  $0 < r < r^*$ . The integrals over  $0 < r < r^*$  for  $\mathcal{F}_{k_1 k_2 k_3}^{l_1 l_2 l_3}$  and  $\Psi_{k_1 k_2 k_3}^{l_1 l_2 l_3}$  are in fact the same, as the integrands coincide in this region; hence the correspondence between  $\mathcal{F}_{k_1 k_2 k_3}^{l_1 l_2 l_3}$  and  $\Psi_{k_1 k_2 k_3}^{l_1 l_2 l_3}$ . (To see this, use eq. (D.5) for  $pr \ll l$  and eq. (D.4) for  $kr \ll l$ , and recall  $\sinh r \approx r$  for  $r \ll 1$ .) In table 1, we show some examples of the correspondence between  $\mathcal{F}_{k_1 k_2 k_3}^{l_1 l_2 l_3}$  and  $\Psi_{k_1 k_2 k_3}^{l_1 l_2 l_3}$ .

$\begin{pmatrix} l_1 & l_2 & l_3 \\ k_1 & k_2 & k_3 \end{pmatrix}$	$\begin{pmatrix} 1 & 1 & 1 \\ 3 & 3 & 3 \end{pmatrix}$	$\begin{pmatrix} 1 & 1 & 1 \\ 5 & 8 & 10 \end{pmatrix}$	$\begin{pmatrix} 1 & 1 & 1 \\ 10 & 10 & 10 \end{pmatrix}$	$\begin{pmatrix} 1 & 1 & 3 \\ 10 & 10 & 10 \end{pmatrix}$	$\begin{pmatrix} 1 & 1 & 10 \\ 10 & 10 & 10 \end{pmatrix}$
$\Psi_{k_1 k_2 k_3}^{l_1 l_2 l_3}$	0.309	0.252	0.309	0.190	0.099
$\mathcal{F}_{k_1 k_2 k_3}^{l_1 l_2 l_3}$	0.279	0.246	0.306	0.185	0.082

**Table 1.** Some numerical values of  $\Psi_{k_1 k_2 k_3}^{l_1 l_2 l_3}$  and  $\mathcal{F}_{k_1 k_2 k_3}^{l_1 l_2 l_3}$ . They agree well when  $1/k_{\min} \ll r^*$  (where  $k_{\min} \equiv \min(|\pm k_1 \pm k_2 \pm k_3|)$ ) and  $l_i/k_i \ll r^*$  for all  $i$  are satisfied.

## D.2 Correspondence with Fourier modes in flat space

Having established the correspondence between the open and flat harmonics, let us now establish the correspondence between coefficients of the open harmonics and those of Fourier expansion in flat space.

Let  $\phi(\mathbf{x})$  be a real function in a 3-dimensional flat space. We shall determine the relation between the multipole expansion coefficients of the flat harmonics,  $\phi_{klm}$ , and the Fourier coefficients,  $\phi(\mathbf{k})$ . We expand  $\phi(\mathbf{x})$  in two way as

$$\phi(\mathbf{x}) = \int_0^\infty dk \sum_{lm} \Psi_{kl}(r) Y_{lm}(\Omega) \phi_{klm}, \quad (\text{D.10})$$

$$= \int \frac{d^3 \mathbf{k}}{(2\pi)^3} e^{i\mathbf{k}\mathbf{x}} \phi(\mathbf{k}), \quad (\text{D.11})$$

where  $r = |\mathbf{x}|$  and  $\Omega$  is the direction of  $\mathbf{x}$ . Using eq. (D.2), reality of  $\phi(\mathbf{x})$ , and the following identity

$$e^{i\mathbf{k}\mathbf{x}} = \sum_{lm} i^l j_l(kr) Y_{lm}^*(\Omega) Y_{lm}(\Omega_k), \quad (\text{D.12})$$

where  $k = |\mathbf{k}|$  and  $\Omega_k$  is the direction of  $\mathbf{k}$ , we find

$$\phi_{klm}^* = \frac{i^l}{(2\pi)^{3/2} k} \int d\Omega_k Y_{lm}(\Omega_k) \phi(\mathbf{k}). \quad (\text{D.13})$$

By using eq. (D.2) and eq. (D.12), we can derive the useful relation

$$i^l \frac{k}{(2\pi)^{3/2}} \int d\Omega_k Y_{lm}(\Omega_k) e^{-i\mathbf{k}\mathbf{x}} = \tilde{Y}_{klm}(\mathbf{x}), \quad (\text{D.14})$$

which will be used below.

## D.3 Power spectrum and bispectrum

We derive the correspondence between the power spectra and bispectra computed with the Fourier coefficients and the coefficients of flat harmonics. The power spectrum and bispectrum for the Fourier modes are given, respectively, by

$$\langle \phi(\mathbf{k}_1) \phi(\mathbf{k}_2^*) \rangle = (2\pi)^3 \delta(\mathbf{k}_1 - \mathbf{k}_2) P(k_1), \quad (\text{D.15})$$

and

$$\langle \phi(\mathbf{k}_1) \phi(\mathbf{k}_2) \phi(\mathbf{k}_3) \rangle = (2\pi)^3 \delta(\mathbf{k}_1 + \mathbf{k}_2 + \mathbf{k}_3) B(k_1, k_2, k_3). \quad (\text{D.16})$$

Using eqs. (D.3), (D.13), (D.14), (D.15), and  $(2\pi)^3\delta(\mathbf{k}_1 - \mathbf{k}_2) = \int d^3\mathbf{x}e^{-i(\mathbf{k}_1 - \mathbf{k}_2)\mathbf{x}}$ , we can re-write the power spectrum for the coefficients of flat harmonics as

$$\begin{aligned} & \left\langle \phi_{k_1 l_1 m_1} \phi_{k_2 l_2 m_2}^* \right\rangle \\ &= \left( \frac{i^{l_1} k_1}{(2\pi)^{3/2}} \int d\Omega_k Y_{l_1 m_1}(\Omega_{k_1}) \right) \left( \frac{(-i)^{l_2} k_2}{(2\pi)^{3/2}} \int d\Omega_{k_2} Y_{l_2 m_2}^*(\Omega_{k_2}) \right) (2\pi)^3 \delta(\mathbf{k}_1 - \mathbf{k}_2) P(k_1) \\ &= \delta(k_1 - k_2) \delta_{l_1 l_2} \delta_{m_1 m_2} P(k_1). \end{aligned} \quad (\text{D.17})$$

Similarly, using eqs. (D.3), (D.13), (D.14), (D.16), and  $(2\pi)^3\delta(\mathbf{k}_1 + \mathbf{k}_2 + \mathbf{k}_3) = \int d^3\mathbf{x}e^{-i(\mathbf{k}_1 + \mathbf{k}_2 + \mathbf{k}_3)\mathbf{x}}$ , we can re-write the bispectrum for the coefficients of flat harmonics as

$$\left\langle \phi_{k_1 l_1 m_1} \phi_{k_2 l_2 m_2} \phi_{k_3 l_3 m_3} \right\rangle = \Psi_{k_1 k_2 k_3}^{l_1 l_2 l_3} \mathcal{G}_{l_1 l_2 l_3}^{m_1 m_2 m_3} B(k_1, k_2, k_3), \quad (\text{D.18})$$

where  $\Psi_{k_1 k_2 k_3}^{l_1 l_2 l_3} \mathcal{G}_{l_1 l_2 l_3}^{m_1 m_2 m_3}$  are defined in eq. (D.8).

Finally, let us find the correspondence between the power spectra and bispectra in open and flat universes. In an open universe,  $P(p_1)$  is defined by  $\langle \phi_{p_1 l_1 m_1}^* \phi_{p_2 l_2 m_2} \rangle = \delta(p_1 - p_2) \delta_{l_1 l_2} \delta_{m_1 m_2} P(p_1)$ , as in section 3, where  $\phi_{p_i l_i m_i}$  are the multipole expansion coefficients with respect to the open harmonics  $Y_{p_i l_i m_i}$ . Comparing this equation with eq. (D.17), we find the correspondence between  $P(p_1)$  and  $P(k_1)$  with identification of  $p_1 \rightarrow k_1$ . Similarly,  $B(p_1, p_2, p_3)$  is defined by  $\langle \phi_{p_1 l_1 m_1} \phi_{p_2 l_2 m_2} \phi_{p_3 l_3 m_3} \rangle = B(p_1, p_2, p_3) \mathcal{F}_{p_1 p_2 p_3}^{l_1 l_2 l_3} \mathcal{G}_{l_1 l_2 l_3}^{m_1 m_2 m_3}$ , as in section D. Comparing this equation with eq. (D.18), and using the correspondence between  $\mathcal{F}_{p_1 p_2 p_3}^{l_1 l_2 l_3}$  and  $\Psi_{k_1 k_2 k_3}^{l_1 l_2 l_3}$  in the sub-curvature approximation, we find the correspondence between  $B(p_1, p_2, p_3)$  and  $B(k_1, k_2, k_3)$  with the identification of  $p_i \rightarrow k_i$ .

## References

- [1] J. R. Gott, *Creation of Open Universes from de Sitter Space*, *Nature* **295** (1982) 304–307.
- [2] J. R. Gott and T. S. Statler, *CONSTRAINTS ON THE FORMATION OF BUBBLE UNIVERSES*, *Phys. Lett.* **B136** (1984) 157–161.
- [3] S. R. Coleman and F. De Luccia, *Gravitational Effects on and of Vacuum Decay*, *Phys. Rev.* **D21** (1980) 3305.
- [4] A. A. Starobinsky, *A New Type of Isotropic Cosmological Models Without Singularity*, *Phys. Lett.* **B91** (1980) 99–102.
- [5] K. Sato, *First Order Phase Transition of a Vacuum and Expansion of the Universe*, *Mon. Not. Roy. Astron. Soc.* **195** (1981) 467–479.
- [6] A. H. Guth, *The Inflationary Universe: A Possible Solution to the Horizon and Flatness Problems*, *Phys. Rev.* **D23** (1981) 347–356.
- [7] A. D. Linde, *A New Inflationary Universe Scenario: A Possible Solution of the Horizon, Flatness, Homogeneity, Isotropy and Primordial Monopole Problems*, *Phys. Lett.* **B108** (1982) 389–393.
- [8] A. Albrecht and P. J. Steinhardt, *Cosmology for Grand Unified Theories with Radiatively Induced Symmetry Breaking*, *Phys. Rev. Lett.* **48** (1982) 1220–1223.
- [9] **WMAP Collaboration** Collaboration, C. Bennett *et. al.*, *Nine-Year Wilkinson Microwave Anisotropy Probe (WMAP) Observations: Final Maps and Results*, [arXiv:1212.5225](https://arxiv.org/abs/1212.5225).

- [10] **WMAP Collaboration** Collaboration, G. Hinshaw *et. al.*, *Nine-Year Wilkinson Microwave Anisotropy Probe (WMAP) Observations: Cosmological Parameter Results*, [arXiv:1212.5226](#).
- [11] **Planck Collaboration** Collaboration, P. Ade *et. al.*, *Planck 2013 results. XVI. Cosmological parameters*, [arXiv:1303.5076](#).
- [12] **Planck Collaboration** Collaboration, P. Ade *et. al.*, *Planck 2013 results. XXII. Constraints on inflation*, [arXiv:1303.5082](#).
- [13] B. Freivogel, M. Kleban, M. Rodriguez Martinez, and L. Susskind, *Observational consequences of a landscape*, *JHEP* **03** (2006) 039, [[hep-th/0505232](#)].
- [14] M. Bucher, A. S. Goldhaber, and N. Turok, *An open universe from inflation*, *Phys. Rev.* **D52** (1995) 3314–3337, [[hep-ph/9411206](#)].
- [15] M. Bucher and J. Cohn, *Primordial gravitational waves from open inflation*, *Phys.Rev.* **D55** (1997) 7461–7479, [[astro-ph/9701117](#)].
- [16] T. Tanaka and M. Sasaki, *The spectrum of gravitational wave perturbations in the one-bubble open inflationary universe*, *Prog. Theor. Phys.* **97** (1997) 243–262, [[astro-ph/9701053](#)].
- [17] K. Yamamoto, M. Sasaki, and T. Tanaka, *Large angle CMB anisotropy in an open universe in the one bubble inflationary scenario*, *Astrophys. J.* **455** (1995) 412–418, [[astro-ph/9501109](#)].
- [18] K. Yamamoto, M. Sasaki, and T. Tanaka, *Quantum fluctuations and CMB anisotropies in one bubble open inflation models*, *Phys.Rev.* **D54** (1996) 5031–5048, [[astro-ph/9605103](#)].
- [19] W. Hu and M. J. White, *Tensor anisotropies in an open universe*, *Astrophys.J.* **486** (1997) L1, [[astro-ph/9701210](#)].
- [20] J. Garcia-Bellido, *Open inflation models and gravitational wave anisotropies in the CMB*, *Phys. Rev.* **D56** (1997) 3225–3237, [[astro-ph/9702211](#)].
- [21] M. Sasaki, T. Tanaka, and Y. Yakushige, *Wall fluctuation modes and tensor CMB anisotropy in open inflation models*, *Phys. Rev.* **D56** (1997) 616–624, [[astro-ph/9702174](#)].
- [22] A. D. Linde, M. Sasaki, and T. Tanaka, *CMB in open inflation*, *Phys. Rev.* **D59** (1999) 123522, [[astro-ph/9901135](#)].
- [23] D. H. Lyth and E. D. Stewart, *Inflationary density perturbations with  $\Omega < 1$* , *Phys. Lett.* **B252** (1990) 336–342.
- [24] B. Ratra and P. J. E. Peebles, *Inflation in an open universe*, *Phys. Rev.* **D52** (1995) 1837–1894.
- [25] B. Ratra and P. J. E. Peebles, *CDM cosmogony in an open universe*, *Astrophys. J.* **432** (1994) L5–L9.
- [26] M. Kamionkowski, B. Ratra, D. N. Spergel, and N. Sugiyama, *CBR anisotropy in an open inflation, CDM cosmogony*, *Astrophys.J.* **434** (1994) L1–L4, [[astro-ph/9406069](#)].
- [27] M. Gorski, Krzysztof, B. Ratra, N. Sugiyama, and A. J. Banday, *COBE - DMR normalized open inflation, CDM cosmogony*, *Astrophys.J.* **444** (1995) L65–L68, [[astro-ph/9502034](#)].
- [28] S. Chang, M. Kleban, and T. S. Levi, *Watching Worlds Collide: Effects on the CMB from Cosmological Bubble Collisions*, *JCAP* **0904** (2009) 025, [[arXiv:0810.5128](#)].
- [29] B. Czech, M. Kleban, K. Larjo, T. S. Levi, and K. Sigurdson, *Polarizing Bubble Collisions*, *JCAP* **1012** (2010) 023, [[arXiv:1006.0832](#)].
- [30] S. M. Feeney, M. C. Johnson, D. J. Mortlock, and H. V. Peiris, *First Observational Tests of Eternal Inflation*, *Phys.Rev.Lett.* **107** (2011) 071301, [[arXiv:1012.1995](#)].
- [31] T. Clunan and D. Seery, *Relics of spatial curvature in the primordial non-gaussianity*, *JCAP* **1001** (2010) 032, [[arXiv:0906.4753](#)].
- [32] A. D. Linde, *A toy model for open inflation*, *Phys. Rev.* **D59** (1999) 023503, [[hep-ph/9807493](#)].

- [33] K. Sugimura, D. Yamauchi, and M. Sasaki, *Multi-field open inflation model and multi-field dynamics in tunneling*, *JCAP* **1201** (2012) 027, [[arXiv:1110.4773](#)].
- [34] D. Yamauchi, A. Linde, A. Naruko, M. Sasaki, and T. Tanaka, *Open inflation in the landscape*, *Phys. Rev.* **D84** (2011) 043513, [[arXiv:1105.2674](#)].
- [35] X. Chen, M.-x. Huang, S. Kachru, and G. Shiu, *Observational signatures and non-Gaussianities of general single field inflation*, *JCAP* **0701** (2007) 002, [[hep-th/0605045](#)].
- [36] R. Holman and A. J. Tolley, *Enhanced Non-Gaussianity from Excited Initial States*, *JCAP* **0805** (2008) 001, [[arXiv:0710.1302](#)].
- [37] P. D. Meerburg, J. P. van der Schaar, and P. S. Corasaniti, *Signatures of Initial State Modifications on Bispectrum Statistics*, *JCAP* **0905** (2009) 018, [[arXiv:0901.4044](#)].
- [38] I. Agullo and L. Parker, *Non-gaussianities and the Stimulated creation of quanta in the inflationary universe*, *Phys.Rev.* **D83** (2011) 063526, [[arXiv:1010.5766](#)].
- [39] J. Ganc, *Calculating the local-type fNL for slow-roll inflation with a non-vacuum initial state*, *Phys.Rev.* **D84** (2011) 063514, [[arXiv:1104.0244](#)].
- [40] D. Chialva, *Signatures of very high energy physics in the squeezed limit of the bispectrum (violation of Maldacena’s condition)*, *JCAP* **1210** (2012) 037, [[arXiv:1108.4203](#)].
- [41] S. Kundu, *Inflation with General Initial Conditions for Scalar Perturbations*, *JCAP* **1202** (2012) 005, [[arXiv:1110.4688](#)].
- [42] A. Dey and S. Paban, *Non-Gaussianities in the Cosmological Perturbation Spectrum due to Primordial Anisotropy*, *JCAP* **1204** (2012) 039, [[arXiv:1106.5840](#)].
- [43] A. Aravind, D. Lorshbough, and S. Paban, *Non-Gaussianity from Excited Initial Inflationary States*, *JHEP* **1307** (2013) 076, [[arXiv:1303.1440](#)].
- [44] J. M. Maldacena, *Non-Gaussian features of primordial fluctuations in single field inflationary models*, *JHEP* **0305** (2003) 013, [[astro-ph/0210603](#)].
- [45] J. Ganc and E. Komatsu, *Scale-dependent bias of galaxies and mu-type distortion of the cosmic microwave background spectrum from single-field inflation with a modified initial state*, *Phys.Rev.* **D86** (2012) 023518, [[arXiv:1204.4241](#)].
- [46] I. Agullo and S. Shandera, *Large non-Gaussian Halo Bias from Single Field Inflation*, *JCAP* **1209** (2012) 007, [[arXiv:1204.4409](#)].
- [47] P. Creminelli, G. D’Amico, M. Musso, and J. Norena, *The (not so) squeezed limit of the primordial 3-point function*, *JCAP* **1111** (2011) 038, [[arXiv:1106.1462](#)].
- [48] X. Chen, *Folded Resonant Non-Gaussianity in General Single Field Inflation*, *JCAP* **1012** (2010) 003, [[arXiv:1008.2485](#)].
- [49] J. Garriga, X. Montes, M. Sasaki, and T. Tanaka, *Canonical quantization of cosmological perturbations in the one-bubble open universe*, *Nucl. Phys.* **B513** (1998) 343–374, [[astro-ph/9706229](#)].
- [50] J. Garriga, X. Montes, M. Sasaki, and T. Tanaka, *Spectrum of cosmological perturbations in the one-bubble open universe*, *Nucl. Phys.* **B551** (1999) 317–373, [[astro-ph/9811257](#)].
- [51] M. Sasaki, T. Tanaka, and K. Yamamoto, *Euclidean vacuum mode functions for a scalar field on open de Sitter space*, *Phys. Rev.* **D51** (1995) 2979–2995, [[gr-qc/9412025](#)].
- [52] R. L. Arnowitt, S. Deser, and C. W. Misner, *The Dynamics of general relativity*, *Gen.Rel.Grav.* **40** (2008) 1997–2027, [[gr-qc/0405109](#)].
- [53] N. D. Birrell and P. C. Davies, *Quantum fields in curved space*. Cambridge University Press, 1982.



- [54] T. S. Bunch and P. C. W. Davies, *Quantum Field Theory in de Sitter Space: Renormalization by Point Splitting*, *Proc. Roy. Soc. Lond.* **A360** (1978) 117–134.
- [55] B. Allen, *Vacuum States in de Sitter Space*, *Phys.Rev.* **D32** (1985) 3136.
- [56] D. H. Lyth and A. Woszczyna, *Large scale perturbations in the open universe*, *Phys. Rev.* **D52** (1995) 3338–3357, [[astro-ph/9501044](#)].
- [57] J. Garcia-Bellido, A. R. Liddle, D. H. Lyth, and D. Wands, *The Open universe Grishchuk-Zeldovich effect*, *Phys.Rev.* **D52** (1995) 6750–6759, [[astro-ph/9508003](#)].
- [58] K. Yamamoto, T. Tanaka, and M. Sasaki, *Particle spectrum created through bubble nucleation and quantum field theory in the Milne Universe*, *Phys. Rev.* **D51** (1995) 2968–2978, [[gr-qc/9412011](#)].
- [59] K. Yamamoto, *Quantum tunneling in multidimensional systems*, *Prog. Theor. Phys.* **91** (1994) 437–452.
- [60] T. Tanaka, M. Sasaki, and K. Yamamoto, *Field theoretic description of quantum fluctuations in multidimensional tunneling approach*, *Phys. Rev.* **D49** (1994) 1039–1046.
- [61] T. Tanaka and M. Sasaki, *Quantum state during and after  $O(4)$  symmetric bubble nucleation with gravitational effects*, *Phys. Rev.* **D50** (1994) 6444–6456, [[gr-qc/9406020](#)].
- [62] K. Sugimura, D. Yamauchi, and M. Sasaki, *Non-Gaussian bubbles in the sky*, *Europhys.Lett.* **100** (2012) 29004, [[arXiv:1208.3937](#)].
- [63] K. Sugimura, *In-in formalism on tunneling background: multi-dimensional quantum mechanics*, *Phys.Rev.* **D88** (2013) 025037, [[arXiv:1306.2207](#)].
- [64] D. S. Park, *Scalar Three-point Functions in a CDL Background*, *JHEP* **1201** (2012) 165, [[arXiv:1111.2858](#)].
- [65] D. Salopek and J. Bond, *Nonlinear evolution of long wavelength metric fluctuations in inflationary models*, *Phys.Rev.* **D42** (1990) 3936–3962.
- [66] E. Komatsu, *The pursuit of non-gaussian fluctuations in the cosmic microwave background*. PhD thesis, Tohoku University, 2002. [astro-ph/0206039](#).
- [67] T. Tanaka and M. Sasaki, *Quantized gravitational waves in the Milne universe*, *Phys. Rev.* **D55** (1997) 6061–6080, [[gr-qc/9610060](#)].